THE INFLUENCE OF CONTROLLED DISTURBANCES ON THE TRANSITION OF POISEUILLE FLOW

Dissertation for the Degree of Ph. D.

MICHIGAN STATE UNIVERSITY

IFTIKHAR RAHMAN MUFTI

1975

This is to certify that the

thesis entitled

THE INFLUENCE OF CONTROLLED DISTURBANCES
ON THE TRANSITION OF POISEUILLE FLOW

presented by

IFTIKHAR RAHMAN MUFTI

has been accepted towards fulfillment
of the requirements for

Ph.D. degree in Mechanical Engineering

Merle C. Potter
Major professor

Date May 13, 1975

O-7639

ABSTRACT

THE INFLUENCE OF CONTROLLED DISTURBANCES
ON THE TRANSITION OF POISEUILLE FLOW

By

Iftikhar Rahman Mufti

An experimental investigation has been done to determine the transition of a plane Poiseuille flow caused by disturbances of finite amplitudes and controlled frequencies. Various non-linear theories which have been developed in the study of finite amplitude disturbances on the transition of a laminar flow are lacking in experimental evidence. The present study was undertaken to furnish the data necessary to support these various non-linear theories. An attempt has been made to draw neutral stability curves for different amplitudes of disturbance in the α-R plane. It has been shown that an increase in the amplitude of the disturbance results in a drop in the critical Reynolds number.

Measurements of wave length of the disturbance wave at different frequencies and different Reynolds numbers have also been performed. It has been observed that regardless of the amplitude and frequency of the

disturbance, the wave speed bears a constant linear relationship with the average speed of flow. In addition, a finite amplitude wave moves three times as fast as the wave with an infinitesimally small amplitude.

All investigations have been conducted for a plane Poiseuille flow. The experimental setup consists of a 24 ft. long channel with an aspect ratio of 78. The fluid used is air and the sinusoidal disturbances are introduced by an electromagnetically driven vibrating ribbon.

THE INFLUENCE OF CONTROLLED DISTURBANCES ON THE TRANSITION OF POISEUILLE FLOW

By

Iftikhar Rahman Mufti

A DISSERTATION

Submitted to
Michigan State University
in partial fulfillment of the requirements
for the degree of

DOCTOR OF PHILOSOPHY

Department of Mechanical Engineering

1975

ACKNOWLEDGMENTS

The author wishes to express his thanks to his major professors, Dr. Merle C. Potter and Dr. Mahlon C. Smith, for their valuable guidance throughout this study. It was through their patience, understanding and personal interest that this work could be accomplished.

Thankful acknowledgment is also extended to Dr. C. Y. Wang, Mathematics Department, and to Dr. D. C. Wiggert, Civil Engineering Department, for their valuable suggestions and for being on my guidance committee.

Sincere appreciation is expressed to Mr. Shuhui Hsu, graduate student, for his assistance in conducting the experiment.

Gratitude is also extended to the National Science Foundation and the Division of Engineering Research, Michigan State University, for their financial support.

The author dedicates this work to his wife Sharlene Teresa and son Shahid Rahman.

TABLE OF CONTENTS

LIST OF TABLES

LIST OF FIGURES

Figure		Page

NOMENCLATURE

A	Amplitude
B	Magnetic flux density
$C = C_r + C_i$	Complex wave speed
I	Ribbon current
$\bar{u}$	Basic parallel flow velocity
R	Reynolds number
u_i	Components of velocity
p	pressure. Also used as a superscript.
x_1	Streamwise coordinate
x_3	Transverse coordinate
y	Coordinate normal to x_1 and x_3
T	Tension in the ribbon
u', v' and w'	x, y, and z components of the disturbance velocity
x, y, z	Coordinate axes
t	time
ψ	Stream function
ϕ	Amplitude function
α	Streamwise wave number
β	Transverse wave number
$i = \sqrt{-1}$	Iota
ω	Frequency of the basic wave

θ	A transformation expressed as $\theta = \alpha x_1 + \beta x_3 + \omega t$
δ_{ij}	Kronecker delta
ρ	Linear mass density of the ribbon
λ	Wave length
∇^2	Laplacian

CHAPTER I

INTRODUCTION

When small disturbances are present in a stream, they have a tendency either to grow or decay in magnitude as they move along the stream. It was Osborn Reynolds (1883) who for the first time recognized that the growth or decay of a disturbance depends on whether the energy is transferred to the disturbance by absorption of energy from the basic flow or is extracted from the disturbance by the damping action of viscosity.

The phenomenon of transition from a laminar flow to a turbulent flow may involve the growth of infinitesimally small disturbances to disturbances having large amplitudes. Whether or not infinitesimally small amplitude disturbances absorb energy from the mean flow field in a channel is a linearized problem described by the famous Orr-Sommerfeld equation (a linearized form of the combined x- and y-component Navier-Stokes equations); but, as the size of the disturbances grows larger, the mathematical analysis necessary to predict the absorption of energy from the mean flow becomes very difficult because of the non-linear nature of the equations involved. Several attempts have been made at obtaining analytical solutions to these non-linear describing equations.

Noether (1921) worked on the non-linear problem of plane Couette flow but considered non-linearity only to the extent of Reynolds stress effect in the equation of mean motion. The terms representing the generation of harmonics of the fundamental disturbance were completely ignored. Heisenberg (1924) considered equations similar (held in balance; unit of viscosity in the cgs = 1 dyne-sec/~~sq~~ centim cm^2 to those used by Noether and included plane Poiseuille flow also in his study. Neither of them, however, gave solutions to the equations developed.

Meksyn and Stuart (1951) gave an approximate method to solve the non-linear equations of Noether and Heisenberg for plane Poiseuille flow and developed an approximate relation between the critical Reynolds number and the amplitude of disturbance. They showed that as the amplitude of disturbance increases, the critical Reynolds number for instability drops exhibiting thereby a sub-critical equilibrium of the disturbance flow.

Stuart (1958) adopted a different approach to study the problem of instability of plane Poiseuille flow. It was based on an energy balance between the rate at which the energy is absorbed from the basic flow (due to the Reynolds stresses) and the rate at which the dissipation of energy of the disturbances takes place by the action of viscosity. For a particular Reynolds number, he assumed that the disturbance velocity has a shape similar to the one given by the linearized theory but the amplitude as an unspecified function of time. Using then the energy balance equation, he showed that for a given wave number, an unstable disturbance amplifies until it reaches an equilibrium amplitude at Reynolds numbers above the critical. Clearly, this contradicted his previous work with Meksyn and so to resolve this basic question, Stuart (1960) adopted still another approach based on Landau's (1944) conjecture that the square of the amplitude ($|A|^2$) of a finite disturbance behaves like the solution of the equation

$$\frac{d|A|^2}{dt} = k_1 \; |A|^2 + k_2|A|^4 \; . \; . \; . \; . \qquad 1.1$$

where "t" is the time and k_1, k_2 . . . are constants. Using only the first two harmonics of the Fourier expansion of the disturbance stream function, in conjunction with Landau's equation (1.1) and the energy balance equations, Stuart developed the following relationship for the change of the disturbance amplitude in a plane Poiseuille flow:

$$\frac{d|A_1|^2}{dt} = 2\alpha c_i \, |A_1|^2 + (k_1 + k_2 + k_3)\,|A_1|^4 \qquad 1.2$$

where c_i represents the growth rate of the disturbance obtained from linear theory and is assumed to be sufficiently small. Stuart observed that the quantities k_1, k_2 and k_3 arise from the following three processes:

1. The distortion of the mean motion (k_1)
2. The generation of the harmonic of the fundamental (k_2)
3. The distortion of the y-dependence of the fundamental (k_3)

k_1 describes the flow of energy to the disturbance due to distortion of the mean flow by the Reynolds stress, and is negative. The flow of energy from the fundamental to the second harmonic is described by k_2 and according to Stuart (1960a) it should be negative. The coefficient k_3 represents the modification of the energy of the fundamental due to distortion of its y-shape. The constant k_3 is large and positive at the critical point and makes the sum $(k_1 + k_2 + k_3)$ positive. In other words, Stuart showed that it is the distortion of the fundamental which is responsible for the sub-critical instability, thus proving the intuitive conclusion that an increase in the amplitude of disturbance results in a drop in the critical Reynolds number.

Watson (1960) developed a perturbation expansion of the non-linear, time-dependent Navier-Stokes equations and solved it to determine the critical Reynolds number for a plane Poiseuille flow subject to finite amplitude disturbances. Even though his technique was different, his conclusions matched with Stuart's regarding the subcritical instability of plane Poiseuille flow.

Reynolds and Potter (1967) developed a formal expansion method to analyze the non-linear development of a 3-D wave in a plane flow and applied it to solve plane Poiseuille and Couette flows. They concluded that relatively weak but finite disturbances markedly reduce the critical Reynolds number.

George and Hellum (1971) solved the non-linear problem by direct numerical integration. Their basic approach was the same as used by the earlier writers, namely by expanding the disturbance stream function in a Fourier series expansion and retaining only the first two harmonics containing unknown coefficients which they defined as being dependent on the stream-wise position in the channel and upon time. They substituted this expression for the disturbance stream function into the N.S. equations expressed in terms of the disturbance stream function and then set the collected coefficients of sine and cosine terms of the respective frequencies equal to zero. This way they obtained a system of coupled non-linear, partial differential equations for the unknown harmonic components and solved this system of equations using a finite difference technique to obtain the desired solutions. Their conclusions were also similar to the one obtained by earlier writers that the disturbances that are stable according to linear theory become unstable with the addition of finite amplitude effects.

J. P. Zahn et al. (1974) solved the non-linear problem of a Plane Poiseuille Flow by expanding the equations describing the flow in Fourier series. They obtained an infinite system of equations for the amplitudes, which were functions of time and of the cross-stream coordinate. The system was truncated after the second harmonic and the resulting equations solved by a finite difference method. They found out that for Reynolds number below 2707, any initial disturbance to the parabolic flow dies away and that for the Reynolds number and the wave number for which the linear theory predicts instability, an initial disturbance of any amplitude gives a particular, steady, finite amplitude solution.

Experimentally, the initial investigation of linear stability theory for a flat plate boundary layer was carried out by G. B. Schubaur and H. K. Skramstad (1947). By inducing oscillations in a boundary layer, they observed the small sinusoidal waves, Tollmein-Schlicting waves, predicted by linear theory. The latter stages of transition of a flat plate boundary layer was examined by H. W. Emmons (1951) and G. B. Schubaur and

P. S. Klebanoff (1956). They observed that the amplified waves became turbulent spots which moved downstream growing steadily in all directions.

Investigations on turbulent bursts in a rectangular channel were conducted by G. C. Sherlin (1960). He determined the growth and propagation speed of turbulent slugs in a rectangular channel with an aspect ratio of 4. The turbulence was induced by injecting a dye and the Reynolds number (based on the average velocity and hydraulic radius) were in the range of 600-2100.

Narayanan and Narayana (1968) extended Sherlin's study for the growth of turbulent slugs and determined that the intermittancy increased with increasing downstream positions at various Reynolds numbers. Their transition, without any artificial disturbances for a channel of aspect ratio 12, occurred at Reynolds number 3000.

Kao and Park (1970) investigated the stability of laminar flow in a rectangular channel with and without artificial excitation. They found the critical Reynolds number (based on average velocity and hydraulic mean radius) as 2600. The fluid used by them was water.

Karnitz (1971) investigated the transition process of flow between parallel plates. He correlated the initial stage of the transition process to linear stability theory. Using a high aspect ratio channel and air as the fluid, he showed that as the velocity disturbance level in the channel was decreased, the transition Reynolds number increased monotonically. For a minimum disturbance level, he obtained a critical Reynolds number of 6,700 for a laminar parabolic flow.

Using the same facility as used by Karnitz, Feliss (1973) studied the mechanism of the transition of flow between parallel plates and obtained a critical Reynolds number of 7,500. His extrapolated curve of Critical Reynolds Number vs Intensity level appears to verify the theoretical value of 7,700.

CHAPTER II

THEORETICAL FOUNDATIONS

Stability Theory for Parallel Shear Flows

The object of our study is to investigate transition of a parallel shear flow caused by disturbances of finite amplitudes; thus, it is desirable to outline a general theoretical development of the theory describing the instability of a fluid flow. This non-linear theory will be formulated for the case of an incompressible fluid. The approach followed is essentially the same as that of Reynolds and Potter [1967].

In a two-dimensional linearized analysis, a fundamental assumption is that the perturbation stream function, ψ, representing deviations of the flow field from the basic steady, parallel laminar flow can be represented by harmonic components, any one of which is of the form

$$\psi = 2 \text{ Re } \{\phi(y) \exp [i\alpha(x - Ct)]\}$$

These harmonics do not interact and therefore their behavior can be studied independently. If this form of the stream function is substituted into the equations of motion and all terms higher than the first order ignored (an infinitesimal amplitude), one obtains the Orr-Sommerfeld problem for the disturbance eigenfunction. It is

$$\{(D^2-\alpha^2)^2 - i\alpha R[(\bar{u}-C)(D^2-\alpha^2) - D^2\bar{u}]\}\phi = 0 \qquad (2.1)$$

$$\phi = D\phi = 0 \text{ at } y = y_1 \text{ and } y_2$$

where

y_1 and y_2 locate the two boundaries of the flow,

$D = \frac{d}{dy}$ and $\bar{u}(y)$ is the basic parallel flow velocity, and

R is the Reynolds number based on the average speed of flow and distance between the parallel plates.

The complex constant $C = C_r + iC_i$ and the wave number α become the eigenvalues of the problem; C_r represents the speed at which the wave propagates downstream and C_i represents the rate at which the wave grows or decays with time. A neutrally stable wave is of particular interest; it occurs when $C_i = 0$. The eigenfunction $\phi(y)$ defines the relative amplitude of the wave.

In a non-linear stability analysis, the disturbances are assumed to have a sufficiently large amplitude that it is not possible to ignore altogether the terms of order higher than one. This may produce three important effects on the motion:

1. The interaction of the basic wave with itself may produce a mean "Reynolds stress" which in turn distorts the mean velocity field.

2. The amplitude of an unstable disturbance may grow until the mean field again becomes stable.

3. Non-linearity may modify the wave speed at which instability occurs.

To study these effects, an expansion method is introduced and is presented below. The development is quite general and covers both two- and three-dimensional cases.

The non-dimensional forms of the basic equations which must be satisfied are

$$\text{Continuity} \quad \frac{\partial u_i}{\partial x_i} = 0, \text{ and} \tag{2.2}$$

$$\text{Momentum} \quad \frac{\partial u_i}{\partial t} + u_j \frac{\partial u_i}{\partial x_j} + \frac{\partial p}{\partial x_i} - \frac{1}{R} \frac{\partial^2 u_i}{\partial x_j \partial x_j} = 0 \tag{2.3}$$

Variables are normalized on suitable characteristic lengths and velocities which remain constant in time.

In a linearized analysis of three-dimensional disturbances, we would assume velocity perturbations of the form

$$u_i' = \hat{u}_i(x_2) \exp [i(\alpha x_1 + \beta x_3 + \omega t)] \exp (at) \tag{2.4}$$

in which $(\omega + ia)$ emerges as a (complex) eigenvalue. The quantity exp (at) allows for growth of the disturbance amplitude. The stability is determined by the sign of "a". In a non-linear analysis, we seek a solution in terms of this basic wave and its harmonics. The following transformation is very helpful in the analysis:

$$\begin{aligned} \theta = \alpha x_1 + \beta x_3 + \omega t; \quad \omega &= \omega(A) \\ A &= A(t) \\ y &= x_2 \end{aligned} \tag{2.5}$$

α and β are streamwise (x_1) and transverse (x_3) wave numbers and ω is the frequency of the basic wave; A is the wave amplitude.

In a two-dimensional case, the transformation to θ - A - y space does not change the number of independent variables, since in the original space the variables are x_1, x_2 and t, but in a three-dimensional case, the number of independent variables reduces from four to three.

In terms of new variables, equations (2.3) and (2.2) become

Momentum

$$\frac{dA}{dt}\frac{\partial u_i}{\partial A} + [\omega + (\frac{d\omega}{dA})t(\frac{dA}{dt}) + \alpha u_1 + \beta u_3]\frac{\partial u_i}{\partial \theta} + u_2 \frac{\partial u_i}{\partial y}$$

$$+ \begin{pmatrix} \alpha \dfrac{\partial p}{\partial \theta} \\ \dfrac{\partial p}{\partial y} \\ \beta \dfrac{\partial p}{\partial \theta} \end{pmatrix} - \frac{1}{R} \left[(\alpha^2 + \beta^2) \frac{\partial^2 u_i}{\partial \theta^2} + \frac{\partial^2 u_i}{\partial y^2} \right] = 0 \tag{2.6}$$

<u>Continuity</u>

$$\frac{\partial}{\partial \theta} (\alpha u_1 + \beta u_3) + \frac{\partial u_2}{\partial y} = 0 \tag{2.7}$$

Select a stream function ψ satisfying continuity. Therefore we have

$$\frac{\partial \psi}{\partial y} = \alpha u_1 + \beta u_3; \quad \frac{\partial \psi}{\partial \theta} = -u_2$$

Now multiply the u_1-momentum equation by α, the u_3-equation by β, and add to obtain an equation involving only ψ and p. Then cross-differentiate the u_2-equation and the combined u_1- and u_3-equations and add to get

$$\frac{dA}{dt} \frac{\partial \zeta}{\partial A} + \left[\omega + \frac{d\omega}{dA}\left(t \frac{dA}{dt}\right) + \frac{\partial \psi}{\partial y}\right] \frac{\partial \zeta}{\partial \theta} - \frac{\partial \psi}{\partial \theta} \frac{\partial \zeta}{\partial y}$$

$$- \frac{1}{R} \left(\frac{\partial^2 \zeta}{\partial y^2} + \kappa^2 \frac{\partial^2 \zeta}{\partial \theta^2} \right) = 0 \tag{2.8}$$

where

$$\zeta = \frac{\partial^2 \psi}{\partial y^2} + \kappa^2 \frac{\partial^2 \psi}{\partial \theta^2}, \text{ and}$$

$$\kappa^2 = \alpha^2 + \beta^2.$$

For the particular case of plane Poiseuille flow, the boundary conditions are

$$\frac{\partial\psi}{\partial\theta} = \frac{\partial\psi}{\partial y} = 0 \text{ at } y = \pm 1$$

With the previous transformations, the resultant equation (2.8) is expressed in terms of one independent variable. The transformations also allowed the eigenvalue ω to appear explicitly in the equation so that it can be expanded along with ψ in the formal treatment.

We next expand the stream function (ψ) in terms of its harmonic components as

$$\psi(A,y,\theta) = \sum_{p=0}^{\infty} \Psi^{(p)}(A,y)e^{ip\theta} + \sum_{p=0}^{\infty} \tilde{\Psi}^{(p)}(A,y)\bar{e}^{ip\theta} \quad (2.9)$$

Summation is carried over all positive integral values of "p" and a tilde (~) denotes the complex conjugate. Substituting in equation (2.8) and separating coefficients of like exponentials, we obtain an infinite set of coupled non-linear partial differential equations for the harmonic amplitudes. The coefficient of $e^{ip\theta}$ gives*

---

*A special summation convention is used. If a superscript occurs twice in one term, a summation is implied, i.e.,

$$\psi^{(j)}\zeta^{(\kappa-j)} = \psi^{(0)}\zeta^{(\kappa)} + \psi^{(1)}\zeta^{(\kappa-1)} + \cdots .$$

The series is terminated if a negative exponent is encountered; i.e., if $\kappa = 2$ in the example of this footnote, the series would contain three terms.

$$\frac{dA}{dt}\frac{\partial Z^{(p)}}{\partial A} + [\omega + \frac{d\omega}{dA}(t\frac{dA}{dt})]ipZ^{(p)} + \frac{1}{1+\delta_{p0}}\left\{\frac{\partial\psi^{(p-j)}}{\partial y}[ijZ^{(j)}]\right.$$

$$+ \frac{\partial\tilde{\psi}^{(j)}}{\partial y}[i(p+j)Z^{(p+j)}] + \frac{\partial\psi^{(p+j)}}{\partial y}[-ij\tilde{Z}^{(j)}] - [i(p-j)\psi^{(p-j)}]\frac{\partial Z^{(j)}}{\partial y}$$

$$\left. - [ij\tilde{\psi}^{(j)}]\frac{\partial Z^{(p+j)}}{\partial y} - [i(p+j)\psi^{(p+j)}]\frac{\partial\tilde{Z}^{(j)}}{\partial y}\right\} \tag{2.10}$$

$$- \frac{1}{R}(\frac{\partial^2}{\partial y^2} - p^2\kappa^2)Z^{(p)} = 0$$

where

$$\delta_{pj} = \begin{cases} 1 & \text{for } p = j \\ 0 & \text{for } p \neq j \end{cases}, \text{ and}$$

$$Z^{(p)} = (\frac{\partial^2}{\partial y^2} - p^2\kappa^2)\psi^{(p)}$$

The boundary conditions necessary in the solution of (2.10) are

$$\psi^{(p)} = \frac{\partial\psi^{(p)}}{\partial y} = 0 \text{ at } y = y_1 \text{ and } y = y_2$$

It is very difficult to solve this infinite set of non-linear coupled equations. However, if the amplitude of the wave is assumed small, it is possible to obtain a solution as a power series in the amplitude A and thereby obtain a sufficient decoupling that a sequential solution is possible. If the amplitude is reduced so that it is infinitesimally small, the solution should represent the Orr-Sommerfeld wave, and the solution for zero amplitude should reduce to the basic laminar flow. Hence, O(A) terms represent the Orr-Sommerfeld fundamental and O(1) terms the laminar flow. In non-linear interaction the terms $O(A^2)$ involve the second harmonic (p = 2) and additional mean terms (p = 0) generated, respectively, by a positive and negative interaction of the fundamental with itself. These in turn interact with the fundamental to produce $O(A^3)$ terms containing the third harmonic (p = 3) and strengthening the fundamental (p = 1). These considerations suggest that we can seek a solution in the form

$$\psi^{(p)}(A,y) = A^n \phi^{(p,n)}(y) \tag{2.11}$$

The double superscript summation convention introduced by Reynolds and Potter [19] represents a sum over all $n \geq p$. Hence, $\psi^{(p)}$ contains no terms of order less than A^p. This way we represent $\psi^{(p)}$ as a series expansion in A and since we wish that the amplitude for infinitesimal A behaves as in linear theory (exponentially), we assume

$$\frac{1}{A}\frac{dA}{dt} = a^{(0)} + Aa^{(1)} + A^2a^{(2)} + \cdots = A^n a^{(n)} \tag{2.12}$$

Constants $a^{(n)}$ have to be determined in some manner; $a^{(0)}$ is an eigenvalue of the linearized analysis; $a^{(1)}$ turns out to be zero and $a^{(2)}$ forms the focus of interest in the non-linear problem.

In case of a flow which is neutrally stable to disturbances of infinitesimal magnitude, $a^{(0)} = 0$ and $a^{(2)}$ determines whether or not a weak disturbance would grow or decay.

Finally, we also represent ω as a power series in A as

$$\omega + \frac{d\omega}{dA}\left(t\,\frac{dA}{dt}\right) = b^{(0)} + Ab^{(1)} \; . \; . \; . = A^n b^{(n)} \tag{2.13}$$

For an equilibrium motion where $dA/dt = 0$, $b^{(n)}$ represents $O(A^n)$ contribution to the frequency of motion. $b^{(0)}$ will represent an eigenvalue of the linearized theory, $b^{(1)}$ turns out to be zero, and $b^{(2)}$ represents change in the oscillation frequency due to the effect of non-linearity.

Substituting equations (2.11)-(2.13) in equation (2.10) and collecting terms of various orders, we obtain an infinite set of equations for $\phi^{(p;n)}$. The coefficient of $A^{(n)}$ yields:

$$\begin{aligned} &ma^{(n-m)}Z^{(p;m)} + b^{(n-m)}ipZ^{(p;m)} + \frac{1}{1+\delta_{po}}\Big(D\phi^{(p-j;n-m)}[ijZ^{(j;m)}] \\ &+ D\tilde{\phi}^{(j;n-m)}[i(p+j)Z^{(p+j;m)}] + D\phi^{(p+j;n-m)}[-ij\tilde{Z}^{(j;m)}] \\ &- [i(p-j)\phi^{(p-j;n-m)}]DZ^{(j;m)} - [-ij\tilde{\phi}^{(j;n-m)}]DZ^{(p+j;m)} \end{aligned} \tag{2.14}$$

$$- [i(p+j)\phi^{(p+j;n-m)}]D\tilde{Z}^{(j;m)}\Big] - \frac{1}{R}(D^2-p^2\kappa^2)Z^{(p;n)} = 0$$

where

$$D = \frac{d}{dy} \quad \text{and}$$

$$Z^{(p;n)} = (D^2 - p^2\kappa^2)\phi^{(p;n)}$$

We can now collect the terms involving $\phi^{(p;n)}$. The basic laminar flow $\bar{u}(y)$ is related to $\phi^{(0;0)}$, the $O(A^0)$ contribution to the zeroeth harmonic, by

$$\bar{u} = \frac{2}{\alpha} D\phi^{(0;0)} = \frac{2}{\alpha} D\tilde{\phi}^{(0;0)} \tag{2.15}$$

When the terms involving $\phi^{(0;0)}$ are represented in terms of $\bar{u}$, equation (2.14) may be written as

$$L_{pn}\phi^{(p;n)} = i\alpha C^{(n-1)}G\delta_{p1} + \frac{H_{pn}}{1+\delta_{p0}} \tag{2.16}$$

δ_{pj} is the Kronecker delta and the operator L_{pn} is expressed as

$$L_{pn} = ip[(-i\,\frac{n}{p}\,a^{(0)} + b^{(0)} + \alpha\bar{u})(D^2 - p^2\kappa^2) - \alpha(D^2\bar{u})]$$
$$\qquad - \frac{1}{R}(D^2 - p^2\kappa^2)^2, \text{ and} \tag{2.17}$$

$$i\alpha C^{(n)} = [a^{(n)} + ib^{(n)}] \tag{2.18}$$

The remaining quantities in equation (2.16) are

$$G = (D^2 - \kappa^2)\phi^{(1;1)} \tag{2.19}$$

$$H_{pn} = -(ma^{[n-m]} + ipb^{[n-m]})(D^2-p^2\kappa^2)\phi^{[p;m]} + F_{pn} \quad \text{and} \tag{2.20}$$

$$\begin{aligned} F_{pn} = &-(D\phi^{[p-j;n-m]})(ij[D^2-j^2\kappa^2]\phi^{[j;m]}) \\ &-(D\tilde{\phi}^{[j;n-m]})\left(i(p+j)[D^2-(p+j)^2\kappa^2]\phi^{[p+j;m]}\right) \\ &-(D\phi^{[p+j;n-m]})(-ij[D^2-j^2\kappa^2]\tilde{\phi}^{[j;m]}) \\ &+\left(i(p-j)\phi^{[p-j;n-m]}\right)(D[D^2-j^2\kappa^2]\phi^{[j;m]}) \\ &+(-ij\,\tilde{\phi}^{[j;n-m]})\left(D[D^2-(p+j)^2\kappa^2]\phi^{[p+j;m]}\right) \\ &+\left(i(p+j)\phi^{[p+j;n-m]}\right)(D[D^2-j^2\kappa^2]\tilde{\phi}^{[j;m]}) \end{aligned} \tag{2.21}$$

The boundary conditions become

$$\phi^{[p;n]} = D\phi^{[p;n]} = 0 \text{ at } y = y_1 \text{ and } y = y_2$$

The bracketed superscripts demand that the quantities in the brackets to the right of the semicolon be greater than or equal to one. When these conditions are applied with $p = 0$, the total mean flow will be held constant. For $p = n = 1$, the right-hand side of equation (2.16) is zero, resulting in the Orr-Sommerfeld equation,

$$\{(a^{(0)}+ib^{(0)}+i\alpha\bar{u})(D^2-\kappa^2) - i\alpha(D^2\bar{u}) - \frac{1}{R}(D^2-\kappa^2)^2\}\phi^{(1;1)} = 0 \tag{2.22}$$

with boundary conditions

$$\phi^{(1;1)} = D\phi^{(1;1)} = 0 \text{ at } y = y_1 \text{ and } y = y_2 .$$

For a two-dimensional motion, where $\kappa = \alpha$, equation (2.22) reduces to the Orr-Sommerfeld problem with $\alpha C = -b^{(0)} + ia^{(0)}$. Thus, if $C(\alpha,\kappa,R) = C^{(0)}$ is the eigenvalue from the linear analysis,

$$b^{(0)} = -\alpha C_r \text{ and } a^{(0)} = \alpha C_i \tag{2.23}$$

The shape of the eigenfunction $\phi^{(1;1)}$ is fixed by equation (2.22), but its amplitude remains arbitrary. If we define A in some particular manner, this definition will fix the amplitude of $\phi^{(1;1)}$ apart from a constant modulus of unity. Alternately, if we arbitrarily normalize $\phi^{(1;1)}$ in some manner, this will define A implicitly. In a plane Poiseuille flow problem, the latter choice is more convenient.

For a plane Poiseuille flow, the mean velocity profile is

$$\bar{u} = \frac{3}{2}\,(1 - y^2) \tag{2.24}$$

The evenness of this profile and of the operators in equation (2.22) allows the eigenfunctions to be separated into families of even and odd functions. If we use the normalizing conditions

$$\phi^{(1;1)}(0) = 1 \text{ for even modes}$$

$$\text{and } D\phi^{(1;1)}(0) = 1 \text{ for odd modes} \tag{2.25}$$

we can solve equation (2.22) for the eigenfunction $\phi^{(1;1)}$ and the eigenvalue C. The solution of equation (2.22) has been achieved by many investigators; the most comprehensive study was made by C. C. Lin [10]. The primary results of interest are presented in a plot of wave number versus Reynolds number, shown in Figure 2.1. The neutral stability curve has a minimum Reynolds number, usually referred to as the critical Reynolds number, of 7,700 at a wave number of 1.02.

Once $\phi^{(1;1)}$ is known, we can move on to the higher order problem. Substituting $\phi^{(1;1)}$ on the right-hand side of equation (2.16) through quantities given in equations (2.19)-(2.21), we can calculate the right-hand sides of these equations when the right-hand side contains either $\phi^{(0;2)}$ or $\phi^{(2;2)}$. The equation then becomes an inhomogeneous linear equation for both of these functions. We can further continue our calculations for n = 3, etc., provided the constants $C^{(n)}$ can be determined along the way.

Reynolds and Potter [1967] have suggested a method to determine the eigenvalues $C^{(n)}$ for small magnitudes of C_i. According to this method, we first have to determine the adjoint function Φ from the adjoint problem

$$\{i\alpha(\bar{u}-C^{(0)})(D^2-\kappa^2) + 2i\alpha(D\bar{u})D - \frac{1}{R}(D^2-\kappa^2)^2\}\Phi = 0 \quad (2.26)$$

$$\Phi = D\Phi = 0 \text{ at } y = y_1 \text{ and } y = y_2$$

Once the adjoint function Φ has been found, $C^{(n)}$ may be found from the equation

$$-i\alpha C^{(n-1)} = a^{(n)} + ib^{(n)} = \frac{\int_{y_1}^{y_2} H_{1n}\Phi dy}{\int_{y_1}^{y_2} G\Phi dy} \quad (2.27)$$

where the functions "G" and "H_{1n}" are given by equations (2.19) and (2.20). The eigenfunctions $\phi^{(p;n)}$ can then be determined from equation (2.16).

A very important conclusion which results from the above analysis is that the constants $C^{(n)}$ vanish for odd n and the functions H_{pn} and $\phi^{(p;n)}$ vanish if (p + n) is odd.

Using numerical techniques, Reynolds and Potter have solved the non-linear problem for the case of a plane Poiseuille flow. Their starting point is the determination of eigenvalues from the solution of the Orr-Sommerfeld problem. These values are then used in the subsequent numerical integration of the higher order differential equations. For the determination of higher order eigenvalues $C^{(n)}$, an iterative scheme has been developed by them. For further details about this method, see their publication [19].

A summary of pertinent constants needed for the evaluation of $C^{(2)}$ for two-dimensional disturbances in a plane Poiseuille flow are shown in Table 2.1. At the critical point on the neutral stability curve, $a^{(2)}$ is positive (+ 19.7) indicating that the finite disturbances actually grow at the critical Reynolds number for a plane Poiseuille flow.

Stuart [26] considered $a^{(2)}$ to be comprised of three components, k_1, k_2 and k_3, given by the equation

$$2a^{(2)} = k_1 + k_2 + k_3 \tag{2.28}$$

Stuart has shown that "k_1" describes the change of the flow of energy to the disturbance due to distortion of mean flow by the Reynolds stresses and is negative; "k_2" which represents the flow of energy from the fundamental to the second harmonic is also negative, while "k_3" represents the modification of the energy of the fundamental due to distortion of its y-shape. In Table 2.1, the values of k_1, k_2 and k_3 are also listed. k_1 and k_2 are both negative while k_3 is large and positive at the critical point indicating that the distortion of the fundamental is responsible for the unstable flow at the critical point of linear theory (see Figure 2.1).

TABLE 2.1.--Summary of Results for Plane Poiseuille Flow.

R	α	C_r	C_i	$a^{(2)}$	$b^{(2)}$	k_1	k_2	k_3
6,000	1.097	0.3773	0.0000	90.90	-206.0	-5.57	-5.71	193
5,000	1.094	0.3896	0.0000	67.35	-172.0	-4.62	-3.97	143
3,848.08*	1.02071	0.39603	0.0000	19.70	-111.0	-2.82	-1.79	44.0
5,000	0.875	0.3516	0.0000	-3.268	-86.0	-2.13	-2.66	-1.74
6,000	0.823	0.3304	0.0000	-7.088	-82.5	-2.04	-3.07	-9.06
4,000	1.02071	0.3394	0.0005	19.89	-113.0	-2.72	-1.85	44.4
3,500	1.02071	0.4026	-0.0015	22.02	-109.0	-3.49	-1.67	49.2

*Critical point. (One-half the channel height is used as the characteristic length.)

More recently, George and Hellums [4] have performed a comparative study of critical curves obtained by various writers. These curves are adjusted to correspond to a common basis of amplitude and Reynolds number and are shown in Figure 2.2. Characteristic length and velocity are the channel half height and maximum velocity, respectively.

Ribbon Oscillations

We wish to insert controlled amplitude and frequency disturbances into the flow at particular locations. A thin ribbon, stretched across the channel and driven electromagnetically, was chosen to provide such disturbances. In the analytical models, sinusoidal disturbances are assumed; thus a sinusoidal, or nearly sinusoidal, disturbance is desired in the experimental situation.

For an electromagnetically driven ribbon, the equation describing the amplitude of ribbon fluctuations is (see Figure 2.3),

$$\frac{\partial^2 y}{\partial t^2} = \frac{T}{\rho}\frac{\partial^2 y}{\partial z^2} + \frac{IB}{\rho}\cos \omega t \tag{2.29}$$

$$y(0) = y(L) = 0$$

where ρ = linear mass density of the ribbon,

B = magnetic flux density,

$I \cos \omega t$ = ribbon current with circular frequency ω, and

T = ribbon tension

Assuming $k = \omega\sqrt{\rho/T}$, a standing wave solution of this equation is

$$y = \frac{IB}{\omega^2 \rho} \frac{1}{\sin (kL)} [\sin (kz) + \sin \{k(L - z)\} \tag{2.30}$$

$$- \sin (kL)] \cos \omega t$$

For resonance,

$$k = \frac{n\pi}{L}; \; n = \pm 1, \pm 2 \; . \; . \; . \; . \tag{2.31}$$

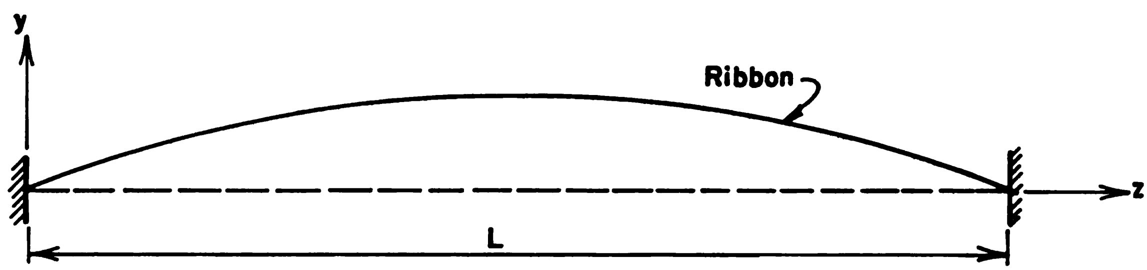

RIBBON DEFLECTION FIG. 2.3

From equation (2.30), the maximum ribbon deflection occurring at the midspan is

$$y_{max} = \frac{IB}{\omega^2 \rho} \frac{1 - \cos \frac{kL}{2}}{\cos \frac{kL}{2}}$$

For a hard drawn copper ribbon of cross-section 3/16" × 0.0051", density = 0.322 lb/cu in, length = 18" and tension = 18 lbs, the resonant frequency is calculated to be 132 Hz. This figure has been confirmed by the experiment.

CHAPTER III

EXPERIMENTAL SETUP

The Flow System

The air channel built for the present study is 24 feet long, 35 inches wide with a constant gap width of 1/2 inch. It consists of two parallel plates, both being hydraulically smooth. The bottom plate is made up of three rolled and polished aluminum sections which are sealed at the joints and polished smooth. The top plate is a series of three acrylic (plexiglass) sections sealed and polished at their joints. The side walls are aluminum strips 1/2" × 1/2" in cross-section and 24 feet long.

Thirteen supporting members consisting of aluminum bars 1" × 1" × 48" are fastened at intervals of 23" across the width of the top plate. Their purpose is to hold the top and bottom plates a constant distance apart of 1/2". The top plate can be adjusted up and down by manipulating bolts in these supporting members. The gap between the plates is accurate to 0.500 ± 0.010 inches.

The entrance region of the air channel consists of a settling chamber 1 foot by 3 feet in cross-section and approximately 5 feet long followed by a 6-foot long streamlined contraction which reduces the 1-foot dimension to the 1/2" gap between the plates. At the exit end of the channel, there is a plenum chamber 8 feet by 5 feet by 4 feet with an exhaust fan assembly attached to it. This draws the air through the assembly resulting in a vacuum at all points in the channel. The details of the flow system are shown in Figures 3.1 and 3.2.

The settling chamber filters out any dust particles from the air before it enters the channel but primarily removes residual large-scale motions from the air, providing a straight, uniform flow. It consists of a fiberglass filter, two honeycomb straw sections completely filled with straws 8-1/4 inches long and 1/4 inch in diameter and a series of 5 screens, 7 inches apart, with mesh sizes of 40, 40, 80, 100 and 120, respectively. The contracting region, beginning 7 inches following the 120 mesh screen, is constructed of sheet metal, wood and fiberglass and is a cantilever-cantilever curve on top and bottom giving zero curvature at both ends of the contraction. The lower part of the contracting region is a strong matrix of wood and fiberglass covered with sheet metal and the upper part is made of fiberglass polished with a paint.

Measurements

Three hot wire probes were placed inside the channel at three different locations, all in the zone of fully developed flow as shown in Figure 3.3. The first probe was placed at mid-height of the channel and about 2 inches upstream of the ribbon. This probe recorded the maximum flow speed in the channel. The distance of the second probe from the base plate was the same as that of the ribbon. It was placed at 2-1/2 inches downstream of the ribbon and recorded the amplitude and frequency of disturbance in the flow at that location. The distance 2-1/2 inches was selected on the basis of observations of the form of the disturbance wave on the oscilloscope. It was observed that at closer distances, the shape of the disturbance wave was distorted and non-sinusoidal. The third probe was placed 27 inches downstream from the ribbon. The output signal from this probe indicated the growth or decay of the disturbance wave.

The complete set of equipment used to collect the data consisted of the following:

(a) Three Disa Type 55D05 constant temperature hot-wire anemometers.

(b) One Disa Type 55D10 linearizer.

(c) One Disa 530 DC Voltmeter.

(d) One Disa 55A60 Calibration unit.

(e) One Disa 55D35 RMS Voltmeter with RMS and RMS squared outputs allowing readings of intensity.

(f) Two TSI 1657 high and low pass filters.

(g) One Quan-Tech 304T wave analyzer with RMS voltage versus frequency output providing a sweep between 0 to 6500 Hz.

(h) One Hewlett-Packard Model 130A double sweep oscilloscope.

(i) One Tektronix 564B fast writing storage oscilloscope coupled with a Tektronix C-40 camera providing a visual and hard copy display.

(j) One Hewlett-Packard low frequency function generator.

(k) One Hewlett-Packard high frequency oscillator.

(l) One Hewlett-Packard Model 5754A Electronic Frequency counter.

(m) One TSI Model 1060 RMS Voltmeter.

(n) One Varian Associates Model F80, X-Y recorder.

(o) One McIntosh Model MC2300 Power Amplifier.

(p) One Kistler Servo Accelerometer Model 305T with range 50 g maximum.

Magnets

Controlled disturbances were introduced by a thin ribbon vibrating in the channel near the lower wall. The ribbon was placed in a magnetic field and the vibrations were caused by passing an alternating current through it. A magnetic field was provided by a series of horseshoe permanent magnets placed above the ribbon outside the channel. Permanent magnets were preferred over electromagnets because of their lighter weight and easy maneuverability. To cause the same effect as that of a high-powered electromagnet as regards the amplitude of ribbon vibrations, higher amplitude current was passed through the ribbon. Intensity of the magnetic field at the ribbon location was 480 gauss.

Ribbon

A 3/16" wide by 0.0051" thick ribbon made of hard drawn copper was used. Hard drawn copper is very strong in tension (tensile strength = 48,000 psi) and yet is a very good conductor of electricity. The use of narrower ribbons was discarded because they produce disturbances that were too small. The possibility of using a round wire was completely ruled out because the disturbances from the eddying wake from the vibrating wire were non-sinusoidal and not controllable.

At first a ribbon length equivalent to the full width of the channel was tried. However, at relatively low speeds, the ribbon would flop back and forth. To avoid the fluttering phenomenon either the tension must be increased or the effective length of the ribbon must be reduced. The ribbon could not resist the high tensions required, thus two intermediate supports of 18 inches apart were provided inside the channel.

The ribbon was stretched between two ends of a brass yoke shown in Figure 3.3. The tension in the ribbon was adjusted prior to insertion into the channel. The yoke and ribbon assembly was then transferred to the test section of the channel.

Sinusoidal A.C. excitation to the ribbon was provided by the schematic shown in Figure 3.4. A sinusoidal signal of chosen frequency from a Hewlet-Packard Function

Generator was first amplified by a McIntosh MC2300 Power Amplifier and then fed to the ribbon.

Hot-Wire Instrumentation

Disa probes, Models 55P11 and 55R01, with 5 μm platinum coated tungsten wire, were used throughout the experiment. Initially, significant drift was noticed at the output signal of the anemometers. This drift was due to one or both of the following reasons:

(1) Oxidation of the probe wire: Oxidation which occurs over a period of time causes the wire properties to change, resulting in output drift. When this occurs the wire should be changed.

(2) Weak batteries: Another cause of the peculiar behavior of the anemometers was the change in the 9 volt batteries contained in the instrument with use. This is particularly noticed if the equipment has to be kept under prolonged experimentation. The use of external 12 volt wet batteries is much more desirable than the internal dry 12 volt batteries that supply current to the hot wire.

An overheating ratio of 1.8 was used for the probe wires.

The anemometer schematic is shown in Figure 3.5.

CHAPTER IV

RESULTS AND DISCUSSION

Introduction

The object of the present study was to investigate transition of a plane Poiseuille flow caused by disturbances of finite amplitudes and controlled frequencies. To do this we intended to map neutral stability curves, for different amplitudes of disturbance, in the α-R plane and thus to verify predictions of various non-linear theories regarding the change in the transition Reynolds number with a change in the amplitude of disturbance.

The theoretical work on non-linear stability of a plane Poiseuille flow with which comparison will be made has been done for the case of a fully developed flow; and in order to render an appropriate comparison between the theoretical and experimental investigations, the tests were performed in the region of fully developed flow between two parallel plates.

The first step in the experiment was, therefore, to examine the velocity profile at the test section. This was done for a set of Reynolds numbers. It was observed that for the working range of flow speeds, the profiles were parabolic at the test section. One of these profiles is shown in Figure 4.1. Small deviations from an actual parabola could be due to the following reasons:

(i) a slight tilt of the probe wire with the horizontal.

(ii) the probe, not being exactly parallel with the direction of flow.

(iii) the position of the probe in the channel being in slight error with the assumed position.

The fact that the theoretical velocity profile is parabolic follows from the solution of steady state Navier-Stokes' equations with no-slip condition at the solid boundaries.

Growing, Neutrally Stable and the Damping Modes

Depending upon the flow speed, the frequency, and the amplitude, a disturbance may grow, be neutrally stable, or decay as it travels along the flow. In a linearized analysis, the amplitude of disturbance is assumed infinitesimally small and a formal solution of the Orr-Sommerfeld equation with suitable boundary conditions gives a relationship between the Reynolds number and the wave number for which the growing, the damping, or the neutrally stable states of the disturbance can be anticipated. C. C. Lin [10] solved the linearized case for a plane Poiseuille flow and determined that the most unstable infinitesimally small amplitude disturbance behaves as neutrally stable for a minimum Reynolds number of 7100. This figure of 7100 was later revised by L. H. Thomas [27] to 7,700.

In a non-linear case, the disturbances have a finite amplitude and, unlike the linear theory, various harmonics are free to interact. Therefore, the simplifications adopted for the linear case cannot be used. The resulting equations are an infinite set of coupled non-linear differential equations. An approximate solution of these equations is possible only if we assume the C_i component of the complex wave speed as being very small in magnitude. The conditions of growth or decay of the disturbance follow from the value of C_i as being positive or negative. Experimentally, this condition is investigated from the output signal of probe 3 shown in Figure 3.3. If the disturbance introduced by the ribbon is damped, the output from probe 3 seen on the oscilloscope screen will not indicate any substantial disturbance in the flow. A growing mode will indicate turbulence, and a neutrally stable mode will show a state of impending burst. This technique was employed to determine the state of neutral stability for disturbances of varying amplitudes and frequencies. Figure 4.2 shows the various stages in which a wave having a growing mode amplifies itself as it travels down the stream. Higher harmonics grow in amplitude and distort the shape of the wave; the eventual stage is turbulence where all frequencies dominate the flow.

According to the non-linear theory, if the speed of the flow is held constant, an increase in the wave number is associated with a monotonic decrease followed by a monotonic increase in the amplitude of a neutrally stable disturbance. This was examined experimentally. Figures 4.3 to 4.8 show the relationship between the intensity of disturbance (which is related to the amplitude of disturbance) introduced by a neutrally stable wave, and the wave number, for various Reynolds numbers. According to these figures, there seems to be no defined pattern in which the intensity of disturbance varies with the wave number. Thus, the theoretical relationship between these two variables appears to be contradicted by the experiment.

To probe further, the cause of this contradiction, a set of frequency spectra for a disturbance wave having a growing mode was taken at various x-locations downstream of the ribbon. Some results of these observations are shown in Figures 4.9 to 4.12. The manner in which the various harmonics of the disturbance wave change their magnitude does not follow any set rule. Higher harmonics grow larger as the wave travels downstream. In Figure 4.11, second harmonic contains even more energy than the fundamental. This behavior of the disturbance wave suggests that:

1. It is not always the fundamental harmonic which triggers turbulence.

2. It is not correct to assume the disturbance wave of finite amplitude to be composed of the basic Orr-Sommerfeld wave and its Fourier components.

To comment on point (1), if energy is transferred to the second harmonic, it may be the one to trigger turbulence and not the fundamental.

To comment on point (2), let us consider a basic property of a Fourier sequence. A Fourier sequence is uniformly convergent unless there are some discontinuities in the function which it represents. In non-linear stability analysis, the Fourier series representing the flow field are considered highly convergent. This is how the series is truncated after the second harmonic with all harmonics higher than the second completely ignored in the analysis. This is in contradiction to the results shown in Figures 4.9 to 4.12. Here, the harmonics higher than the second contain substantial amounts of energy and cannot be ignored. Figure 4.11 shows a situation where the second harmonic is even more important than the fundamental in bringing about the state of turbulence. This suggests that:

1. Harmonics higher than the second are not negligible
2. The use of Fourier series in the representation of the disturbance flow field may not, after all, be an acceptable step.

Figure 4.13 represents neutral stability curves for various amplitudes of disturbance in the α-R plane.

Observations were extended to disturbances having very high frequencies. A study of this figure suggests that there is hardly any relationship between the theoretical and experimental curves (see Figure 2.1 for theoretical curves). Nevertheless, one thing is confirmed; that is, as the amplitude of disturbance increases, the critical Reynolds number (or the minimum Reynolds number), which corresponds to the initial burst, decreases. The idea that all zones above and below the well-defined theoretical neutral stability loop (Figure 2.1) in the α-R plane are stable seems invalid. There are instabilities in the flow field where theory predicts none.

Measurements of Wave-Length

The wave speed is an important parameter of this study and is determined by measuring the wavelength of the disturbance. This was done for various frequencies of disturbance at different speeds of channel flow.

A double sweep oscilloscope was used for measuring the wave length. The input to the ribbon from the frequency oscillator was connected to the X-terminals of the oscilloscope and the output from the wire was connected to the Y-terminals. A stationary Lissajous figure consisting of a single closed loop was obtained since the frequencies of both the input and the output were the same. As the distance between the ribbon and the hotwire was changed, this figure changed from a straight line to an ellipse, then to a circle, again to an ellipse, and finally to a straight line inclined 90° to the first straight line. This indicated that the phase between the input to the ribbon and output from the wire had changed by 180° and that the change in the spacing between the ribbon and the wire was half the wave length. Figure 4.14 shows different stages of Lissajous figures as seen on the oscilloscope screen.

The wave speed was then calculated by multiplying the wave length by the frequency of oscillations. Figure 4.15 shows a plot between the normalized wave speed and the frequency of disturbances. Normalization has been done with reference to the average speed of flow. Two important conclusions can be drawn from Figure 4.15.

1. $\frac{U_{wave}}{\bar{U}}$ is invariant with respect to frequency of disturbances.

2. The speed of a wave with finite amplitude is 1.2 times the average speed of flow. This is approximately 3 times the speed of a wave with infinitesimally small amplitude as predicted by linearized theory.

Amplitude of Imposed Disturbance Versus Depth

Figure 4.16 shows the amplitude distribution (measured in terms of percent intensity of fluctuations $\frac{\sqrt{u'^2}}{\bar{U}}$ x 100) over the lower half of the channel. At a constant channel speed, the experiment was repeated for different frequencies of disturbance. Measurements of intensity of fluctuations were conducted at the location x = 2 1/2" and z = +3 (see Figure 4.17 for reference coordinates). It was observed that the intensity of the disturbance remains maximum in the vicinity of the "critical layer."* In a plane Poiseuille flow between the two parallel plates, there are two critical layers symmetrically located on either side of the central core. In Figures 4.18 and 4.19, it is demonstrated that even though the location of the induced disturbance may be near the lower or the upper plate, the intensity of the disturbance grows to a maximum as we move towards the critical layer. This behavior of the finite amplitude disturbances matches with the behavior of infinitesimally small magnitude disturbances of the linearized theory and Lin's statement (1958) "that for disturbances in a parallel flow, all the harmonic components simultaneously become important around the critical layer" is verified.

Figure 4.20 shows the amplitude distribution along the depth of the channel when the disturbance is introduced at the mid-height of the channel. Unlike the critical layer, the middle layer is highly stable and therefore, as long as the disturbance does not have a very high initial

---

*The critical layer was defined by C. C. Lin to be the layer on either of the points where $C_r = U$ as predicted by linear theory. For channel flow this occurs at $y/h = \pm 0.9$.

amplitude, it is damped before it enters the sensitive zones of the critical layers.

Transition Reynolds Number

Figure 4.21 shows a plot of percentage intensity of disturbance versus the transition Reynolds number. The intensity of disturbance was measured at a constant location (x = 2.5"; y = -0.14" and z = +3") where the x, y, z coordinate system is shown in Figure 4.17. Disturbances of varying frequency were introduced by the ribbon. Figure 4.21 demonstrates that as the Reynolds number is decreased, higher amplitude disturbances are required to bring about transition.

Effect of Ribbon Size and Supports

In order to determine the effect of the ribbon size and its intermediate supports on the data, two separate sets of observations were taken, one with the original ribbon replaced by another ribbon of a different cross-section and the second with the intermediate supports (shown in Figure 3.3) replaced by two 3" long aerofoil supports. Figure 4.22 shows a plot of the RMS value of the output voltage from probe 2 (Figure 3.3) versus frequency of disturbance for a constant speed of the channel flow. For both ribbons, the RMS corresponds to the neutrally stable modes.

Sharp similarity between the two curves suggests that the ribbon size does not affect the behavior of the disturbance wave. The reason for an earlier transition in the case of a wider ribbon could be due to the greater amount of circulation introduced into the flow by the wider ribbon.

Table 4.1 shows the RMS of the output voltage from probe 2 for two different types of intermediate supports. Here again, the channel speed was held constant and the RMS was measured for neutrally stable modes. The type of intermediate supports has little effect on the experiment.

TABLE 4.1.--R.M.S. Output With Bar and Aerofoil Supports.

Bar Supports		Aerofoil Supports	
Frequency (HZ)	RMS	Frequency (HZ)	RMS
100	.023	100	.026
120	.0225	120	.022
200	.013	200	.0165
250	.0046	250	.0067
300	.0034	300	.0068
350	.00115	350	.0036
400	.00205	400	.0024

Measurement of v'-component of the Disturbance Velocity

Theoretically, for a symmetrical velocity profile like that of a plane Poiseuille flow, the v'-component of the disturbance velocity at the middle height ($y = 0$) of the channel should be zero. This was examined experimentally by using an x-probe. The average speed of flow in the channel was maintained constant at 18 fps (Reynolds number = 4687), and a disturbance with a growing mode and having a frequency of 200 Hz was introduced by the ribbon. Observations were taken at different x and z locations shown in Table 4.2. Note that in this instance, a slight decay occurs in the value of u' between 2.5" and 4" before it finally grows.

TABLE 4.2.--u' and v' Components of the Disturbance Flow.

x (inches) (Distance downstream of the ribbon	z (inches) Lateral distance from the centerline of the channel	u' (fps)	v' (fps)
2.5"	+3	1.22	negligibly small
	+2	1.28	negligibly small
	+1	1.26	negligibly small
	0	1.15	negligibly small
	-1	1.23	negligibly small
	-2	1.26	negligibly small
	-3	1.32	negligibly small
4"	+3	0.83	1.35×10^{-5}
	+2	0.78	4.06×10^{-4}
	+1	0.75	negligibly small
	0	0.69	negligibly small
	-1	0.77	negligibly small
	-2	0.81	negligibly small
	-3	0.68	negligibly small

It is evident from the results that the v'-component of the disturbance velocity is negligibly small.

Conclusions

The following conclusions are drawn from the present study:

1. Marked differences between the shapes of the theoretical neutral stability curve for finite amplitude disturbances shown in Figure 2.1 and the experimental curves shown in Figure 3.1 studied in conjunction with frequency spectra shown in Figures 4.9 to 4.12 suggest that the imposed disturbances become three-dimensional downstream of the point at which they are introduced. Therefore, in order to investigate theoretically a flow containing finite amplitude disturbances, we should consider three-dimensional disturbances in place of two-dimensional ones.

2. The transition Reynolds number which corresponds to the state of an impending burst (also called the critical Reynolds number) decreases as the amplitude of the disturbance is increased.

3. It is not necessarily the fundamental frequency introduced into the flow which triggers turbulence, as is obvious from Figures 4.9 to 4.12. Energy may be transferred to higher harmonics which then grow and cause transition.

4. The speed of a wave with a finite amplitude is 1.2 times the average speed of flow. This is approximately three times the speed of a wave with an infinitesimally small amplitude as predicted by linearized theory.

5. Regardless of the location where a disturbance is introduced in a plane Poiseuille flow, the amplitude of the disturbance is maximum in the vicinity of the "critical layer" near each wall.

Suggestions for Future Research

One way to interpret three-dimensionality of the disturbance wave could be due to an interaction of the induced disturbance with the noise inherent in the flow. Two steps are recommended in this regard:

1. Precise measurements of w'-component of the disturbance at various locations in the flow field.
2. Reduce the noise level of the channel flow to a minimum and repeat the whole set of data to examine whether or not the three-dimensionality of the disturbance wave still persists.

Another useful study would be to investigate transition caused by finite amplitude disturbances in the entrance region and to relate it with the findings of the linearized analysis.

In the present study we could not determine the contribution of sound generated by the vibrating ribbon in the measured amplitude of the disturbance. If the sound effect could be sifted out from the effect of mechanical vibrations of the ribbon, we may possibly get to the causes of three-dimensional behavior of the disturbance wave. Even though it would not be possible to superimpose one effect on to the other due to their non-linear nature, it may be a step forward in this type of research.

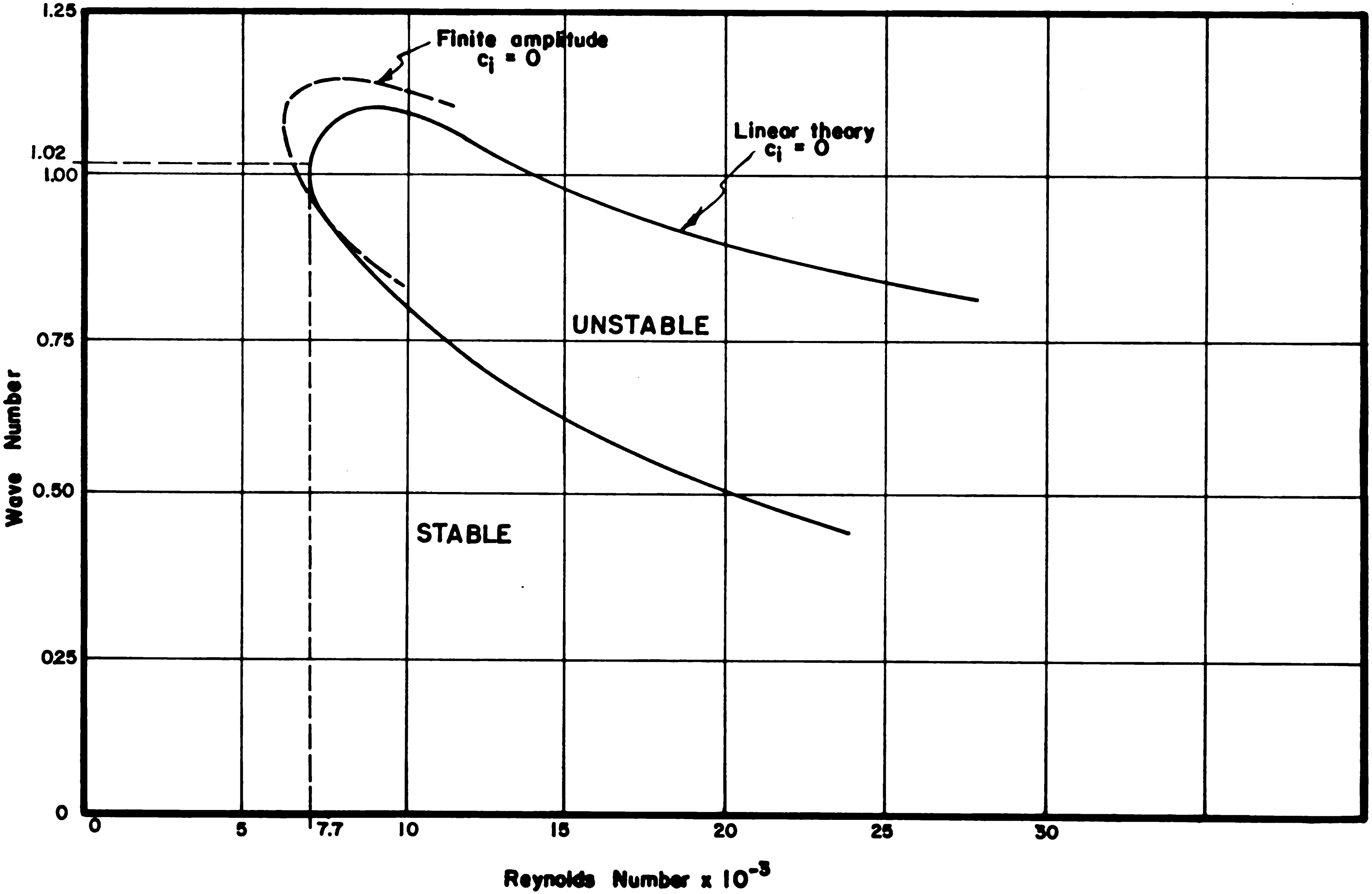

STABILITY CURVE FOR A PLANE POISEUILLE FLOW (Figure 2.1)

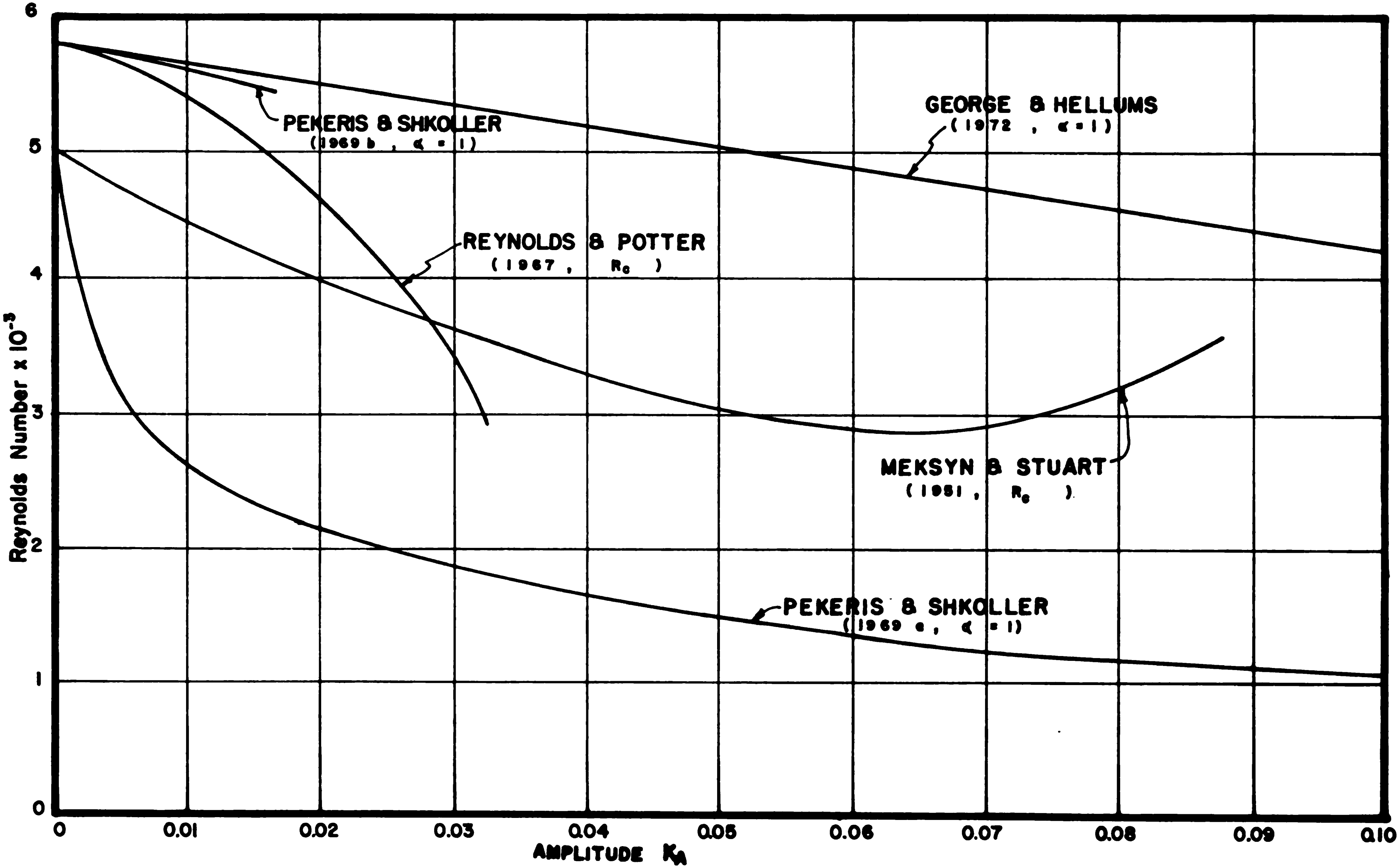

CRITICAL CURVES FOR PLANE POISEUILLE FLOW FIG. 2.2

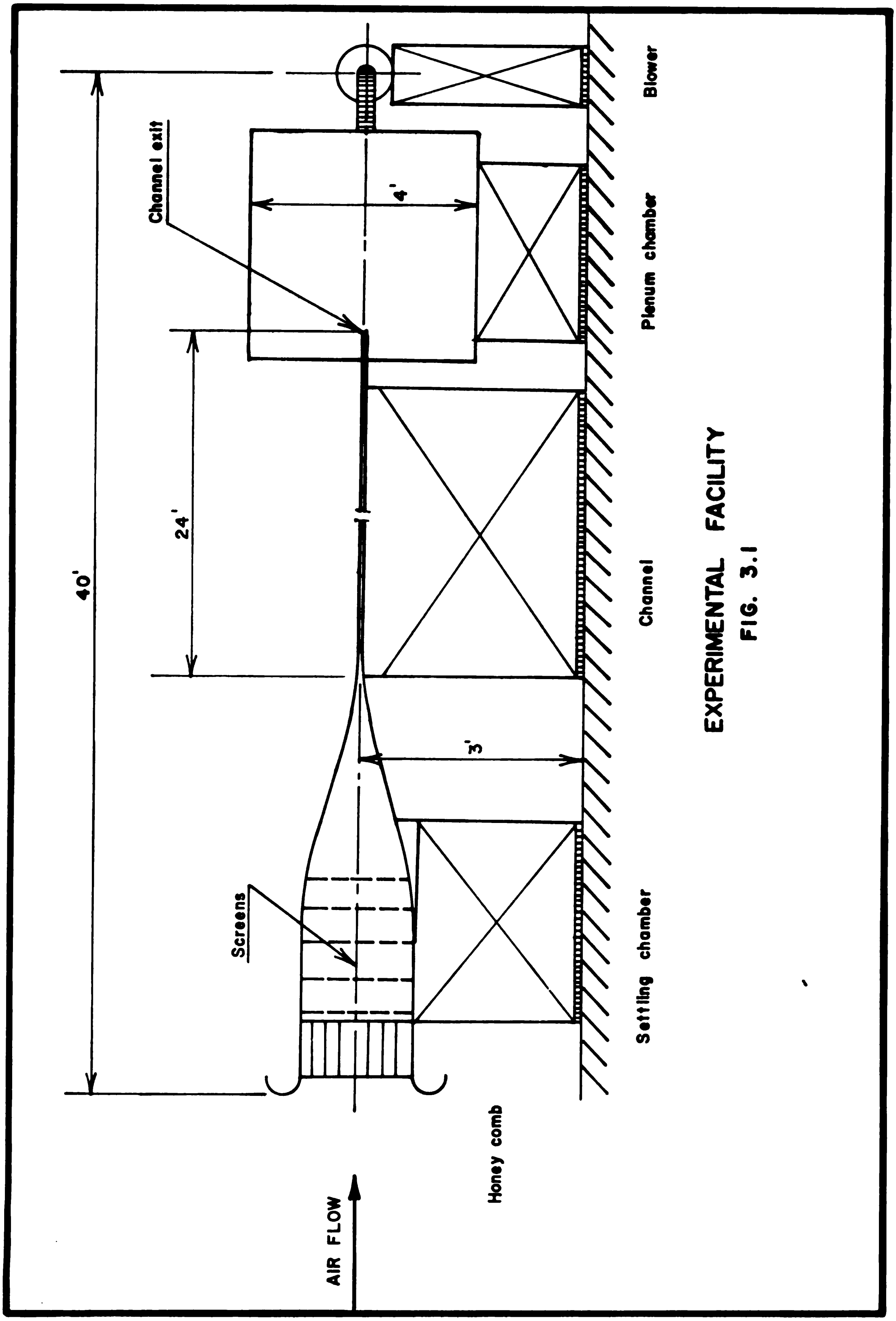

EXPERIMENTAL FACILITY
FIG. 3.1

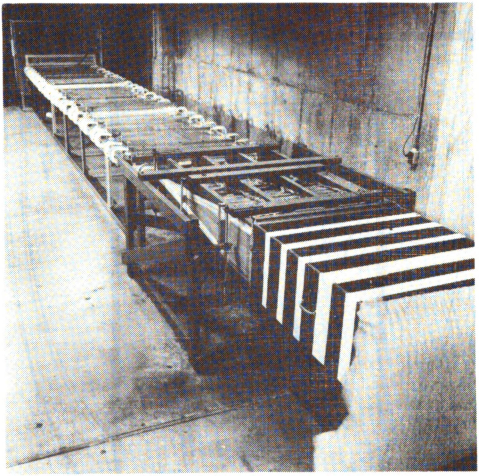

PHOTOGRAPH OF THE CHANNEL FIG. 3.2

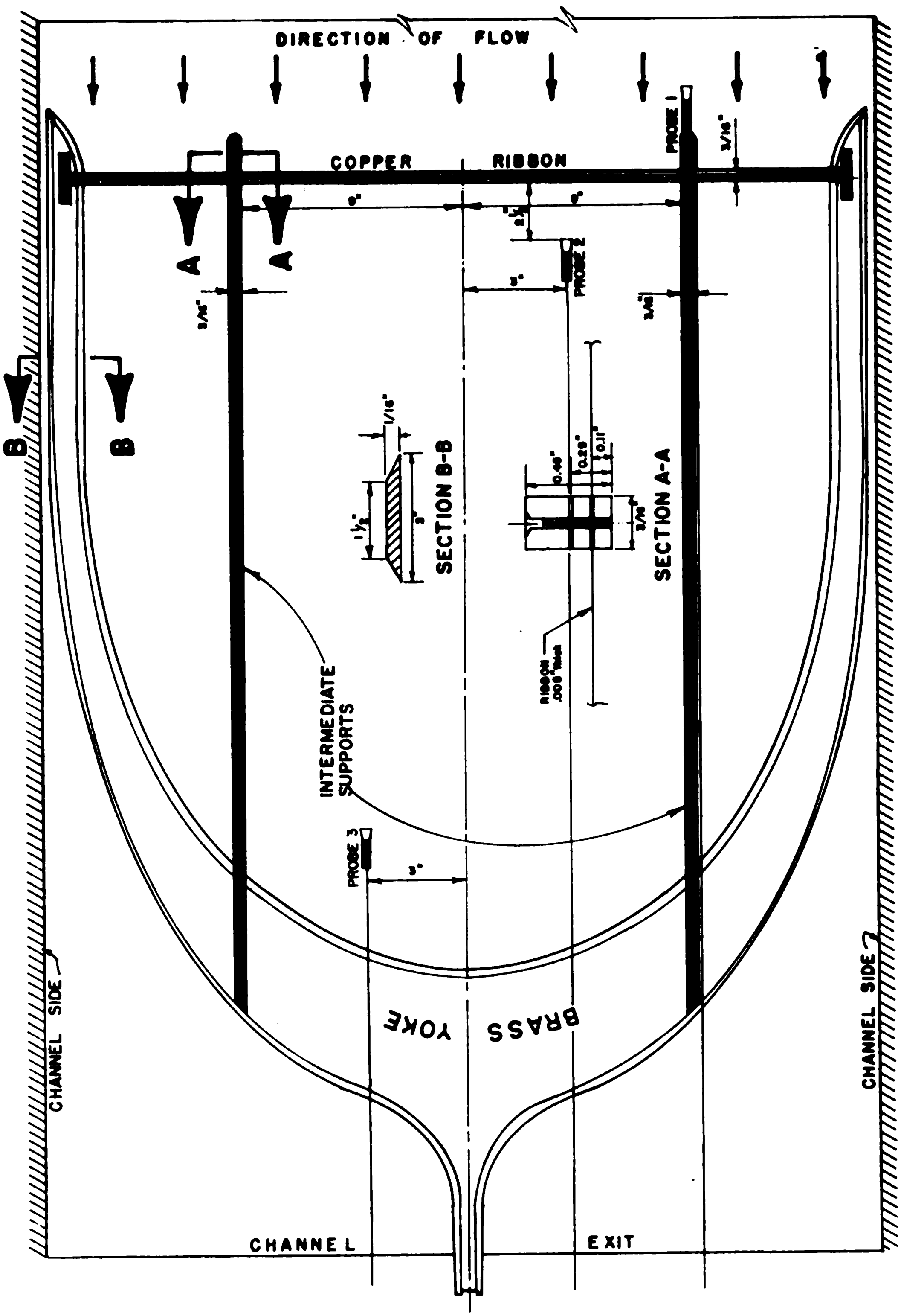

RIBBON SUPPORT

FIGURE 3.3

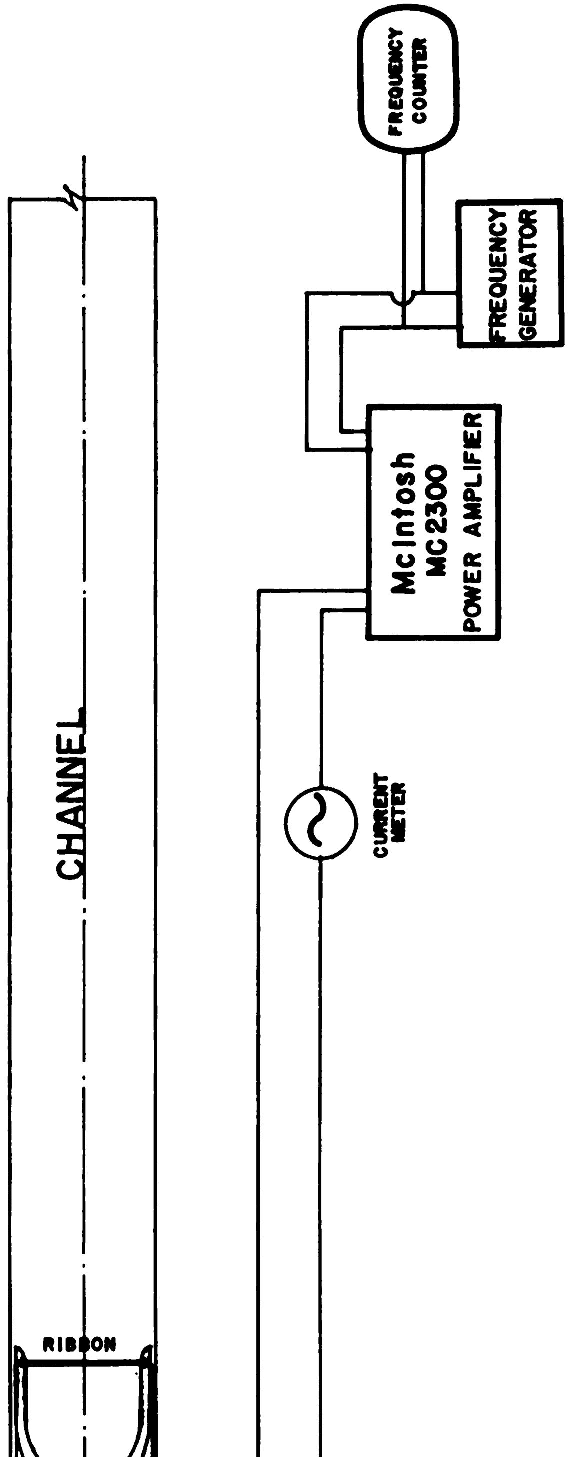

ELECTRICAL SCHEMATIC FOR AMPLITUDE & FREQUENCY CONTROL
(FIGURE 3.4)

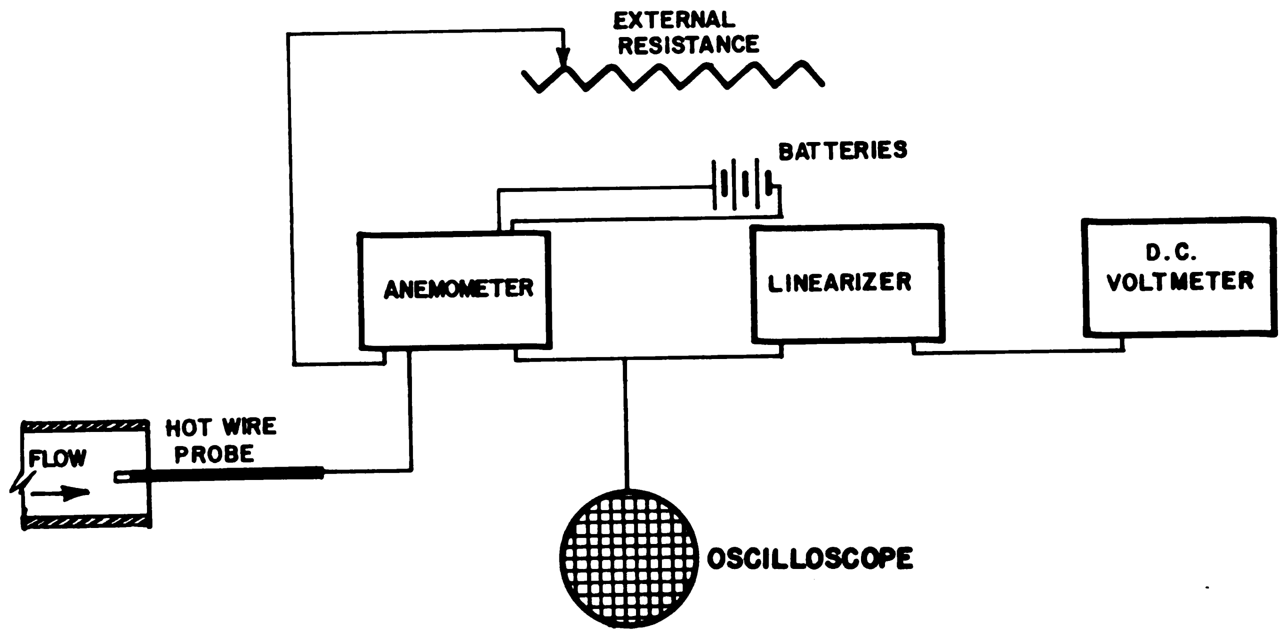

ELECTRICAL SCHEMATIC FOR FLOW MEASUREMENT

FIG. 3.5

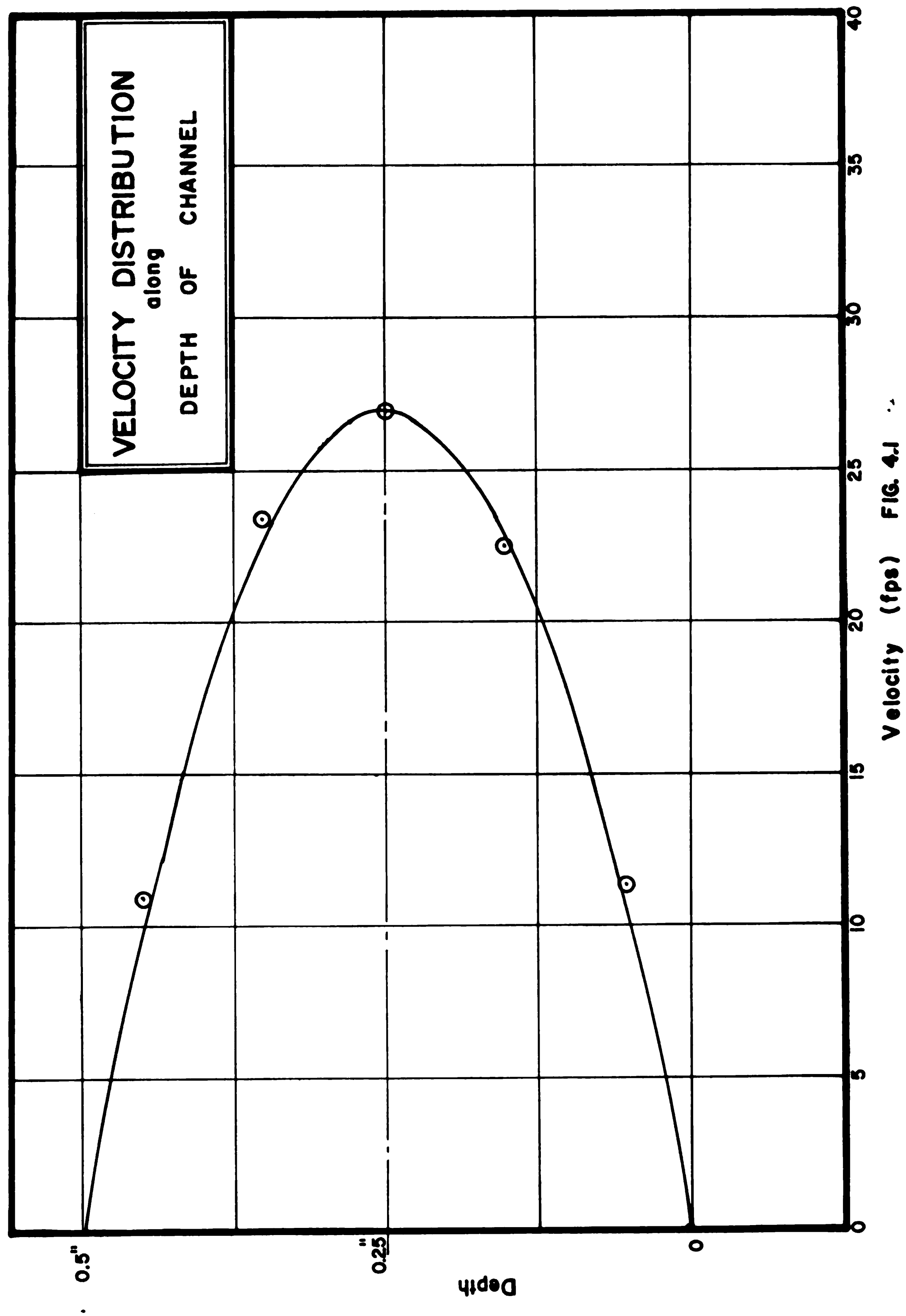
VELOCITY DISTRIBUTION
along
DEPTH OF CHANNEL
Velocity (fps)
Depth
0
5
10
15
20
25
30
35
40
0.5"
0.25"
0

FIG. 4.1

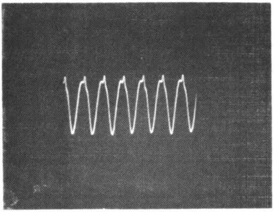

No. 1 X = 1"

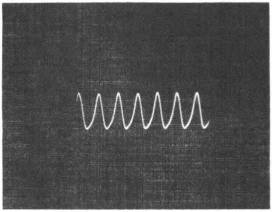

No. 2 X = 2.5"

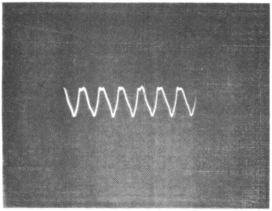

No. 3 X = 4"

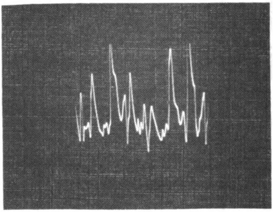

No. 4 X = 10"

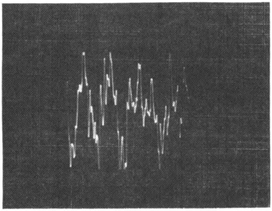

No. 5 X = 16"

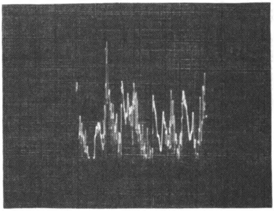

No. 6 X = 24"

STAGES OF GROWTH OF WAVE MOVING IN THE DIRECTION OF FLOW FIG. 4.2

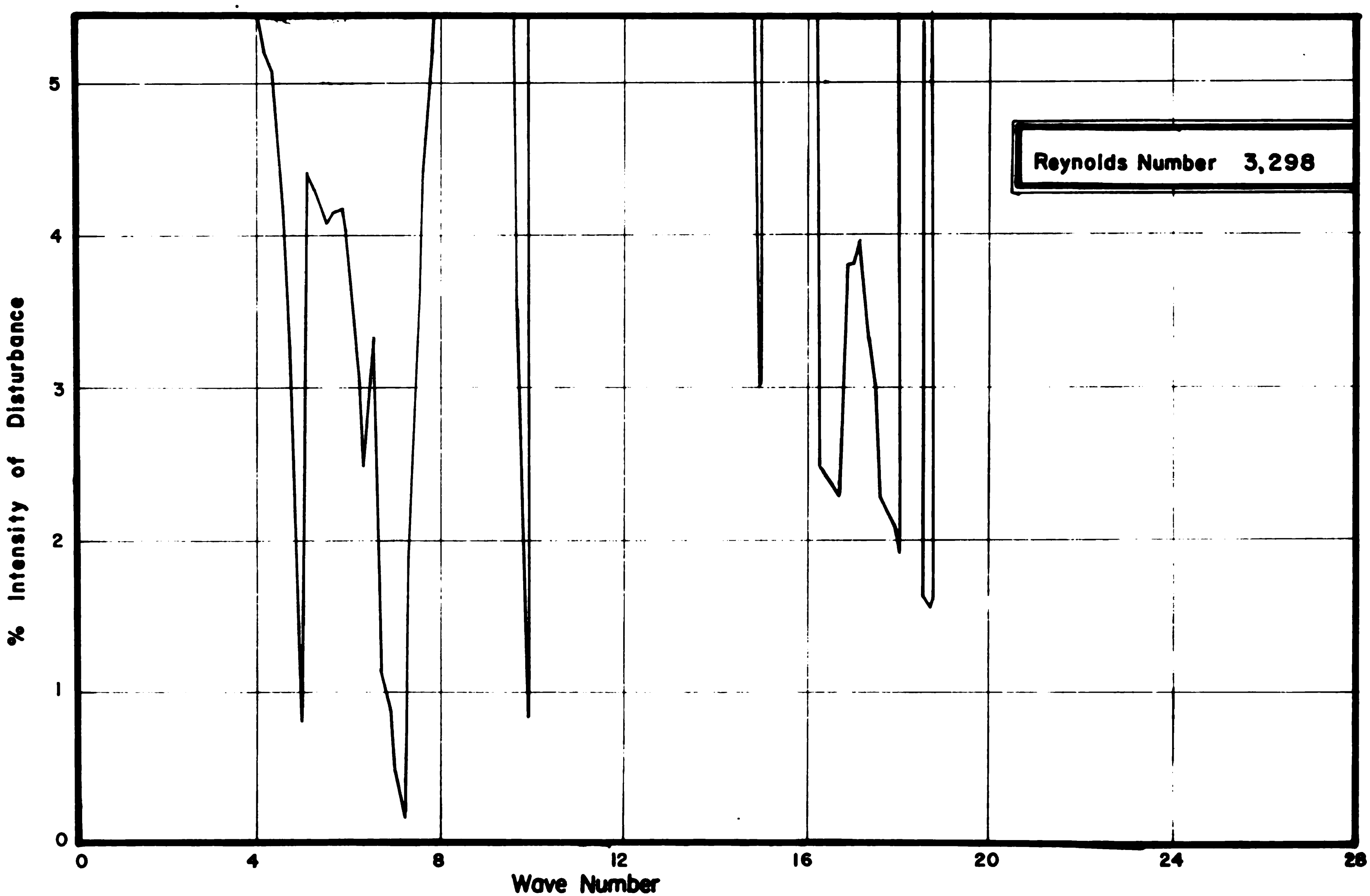

VARIATION OF INTENSITY WITH WAVE NUMBER FIG.4.3

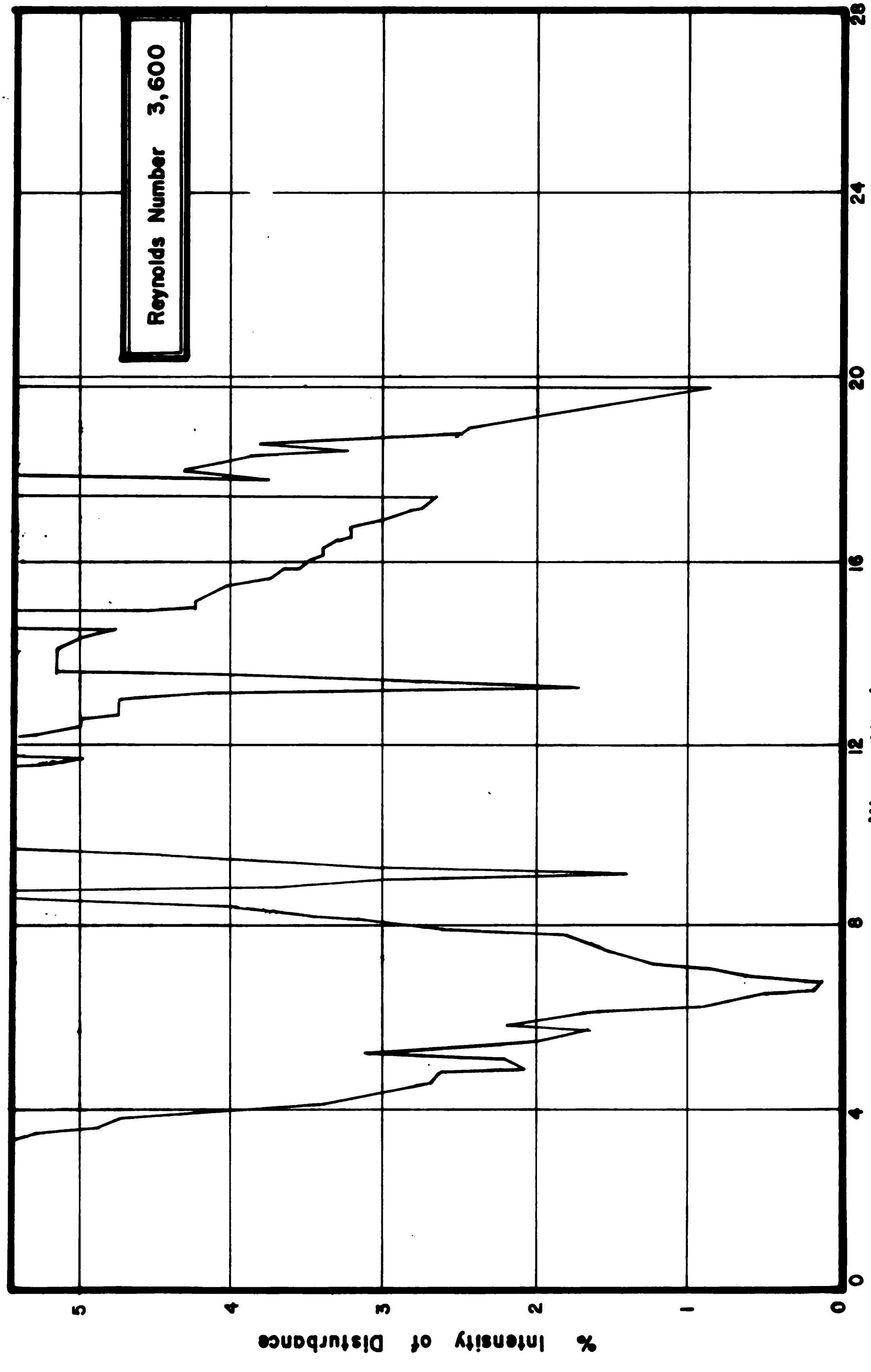

VARIATION OF INTENSITY WITH WAVE NUMBER FIG. 4.4

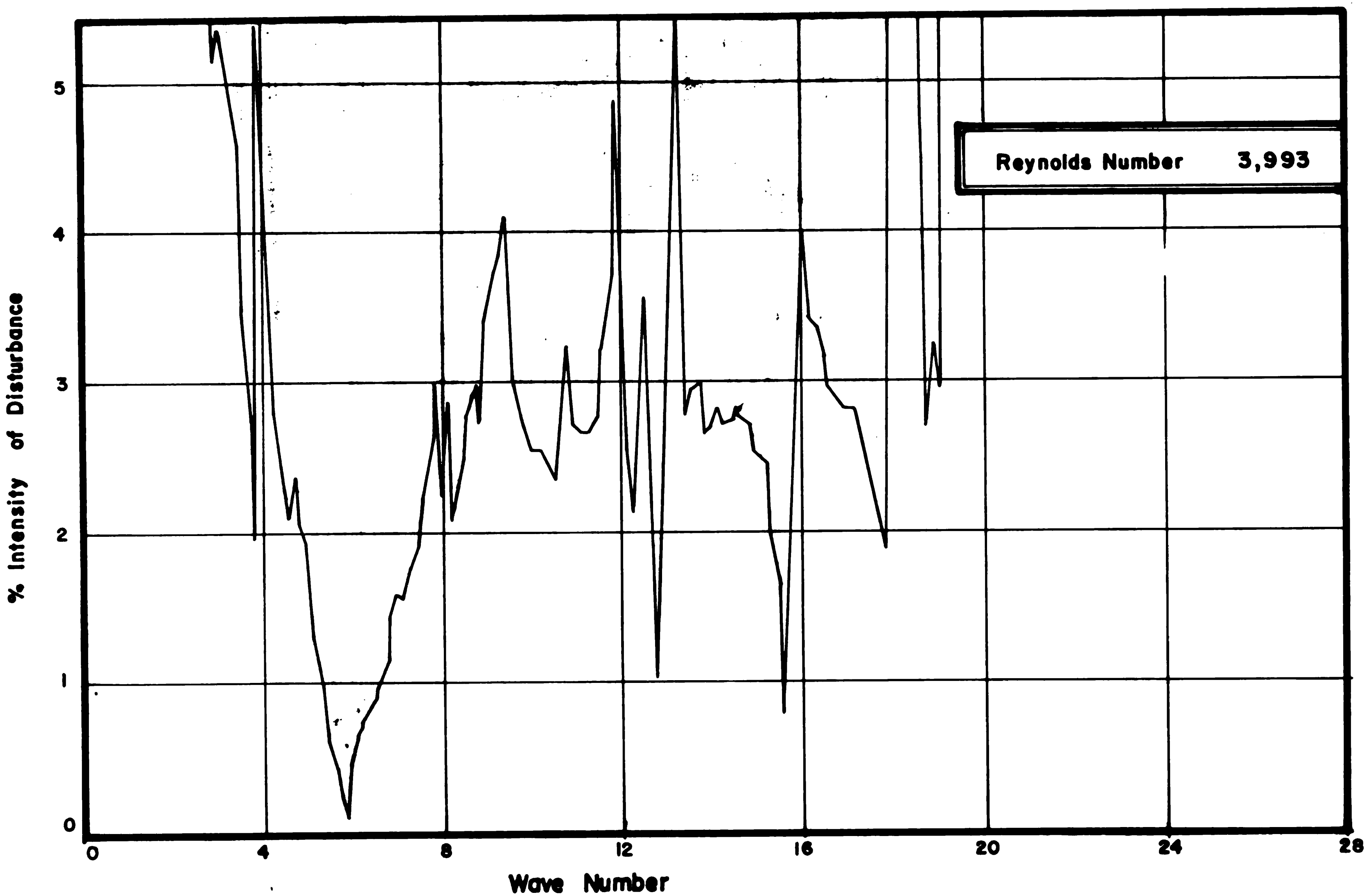

VARIATION OF INTENSITY WITH WAVE NUMBER FIG. 4.5

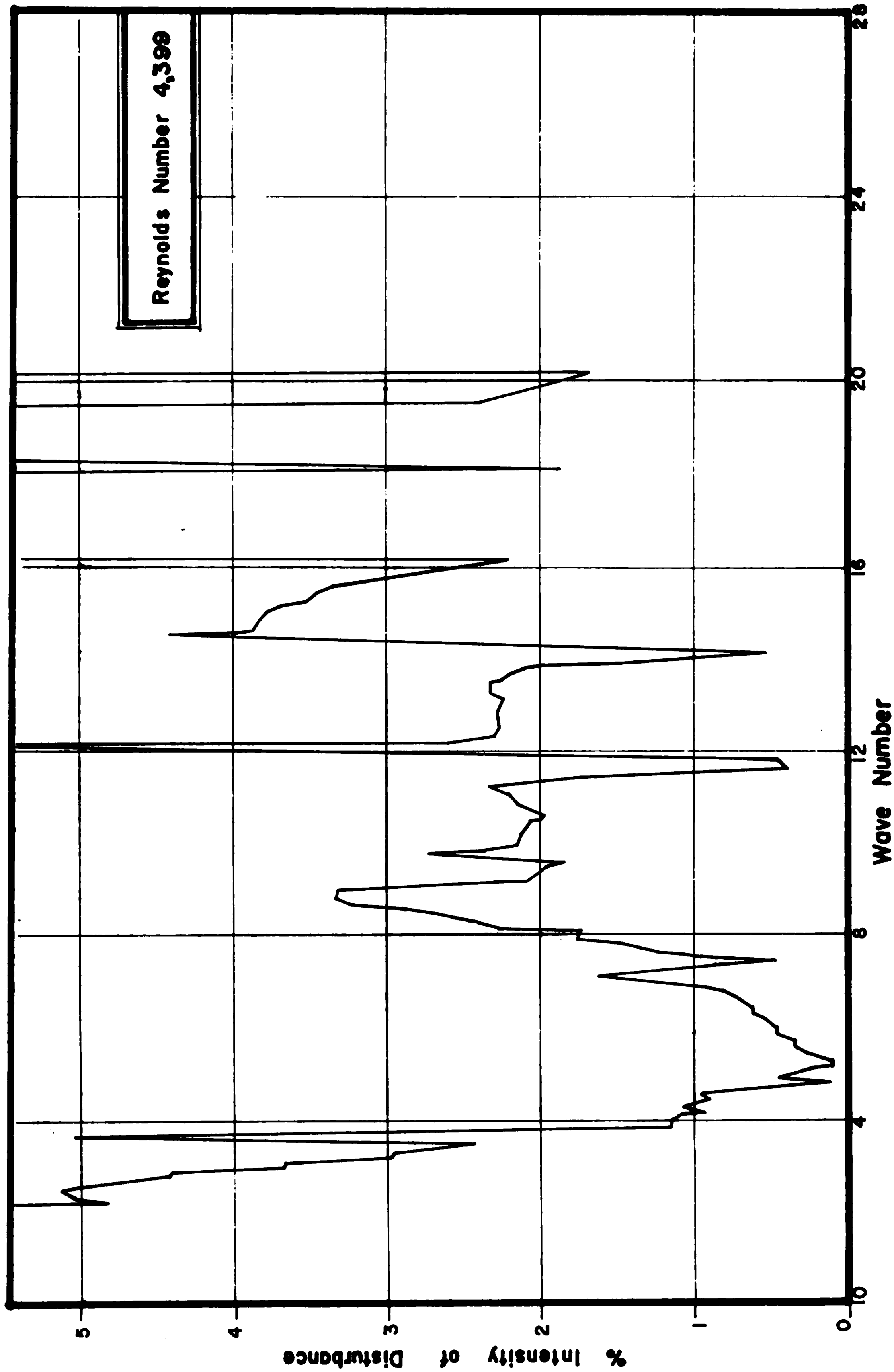

VARIATION OF INTENSITY WITH WAVE NUMBER FIG. 4.6

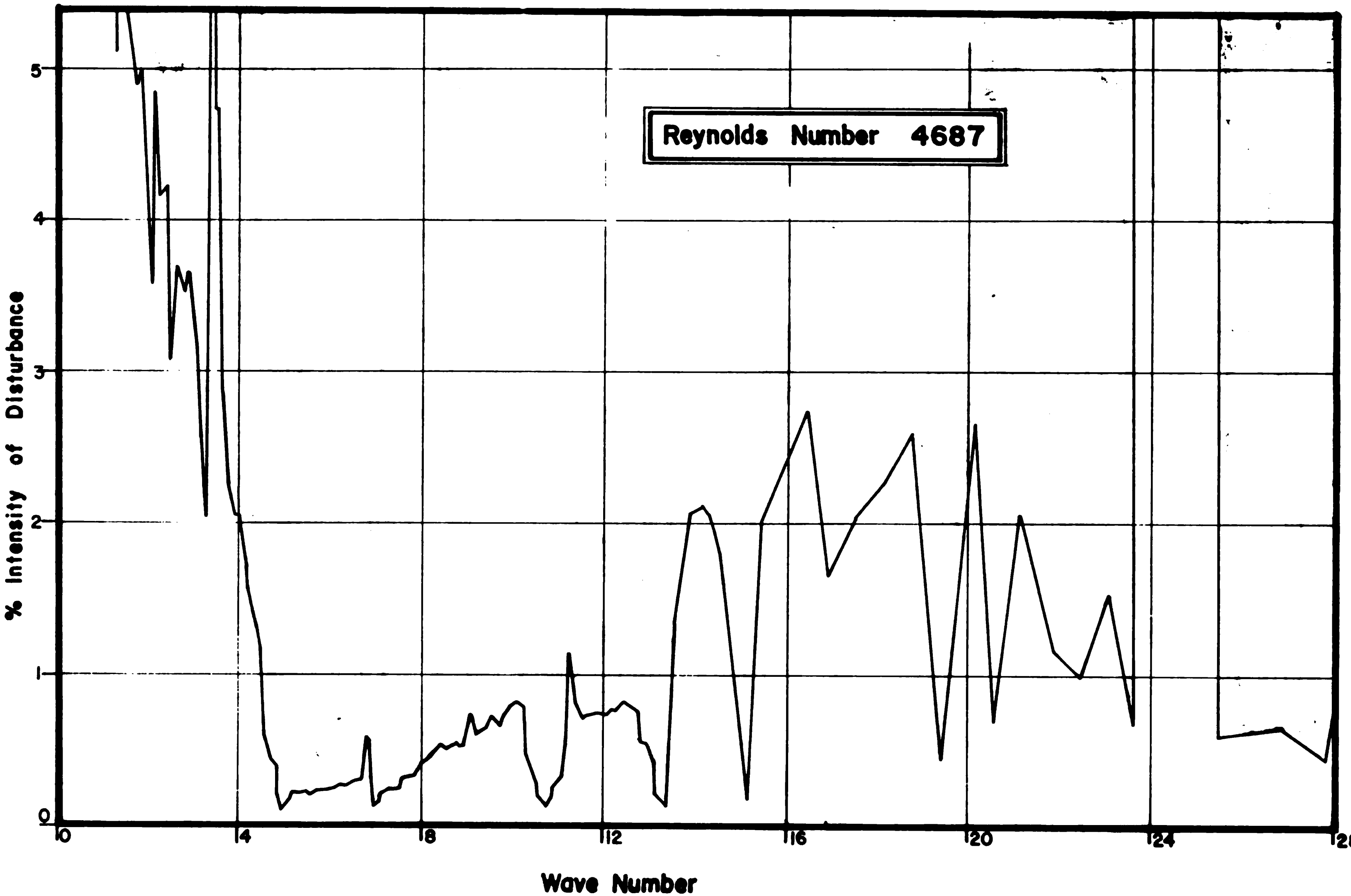

VARIATION OF INTENSITY WITH WAVE NUMBER FIG. 4.7

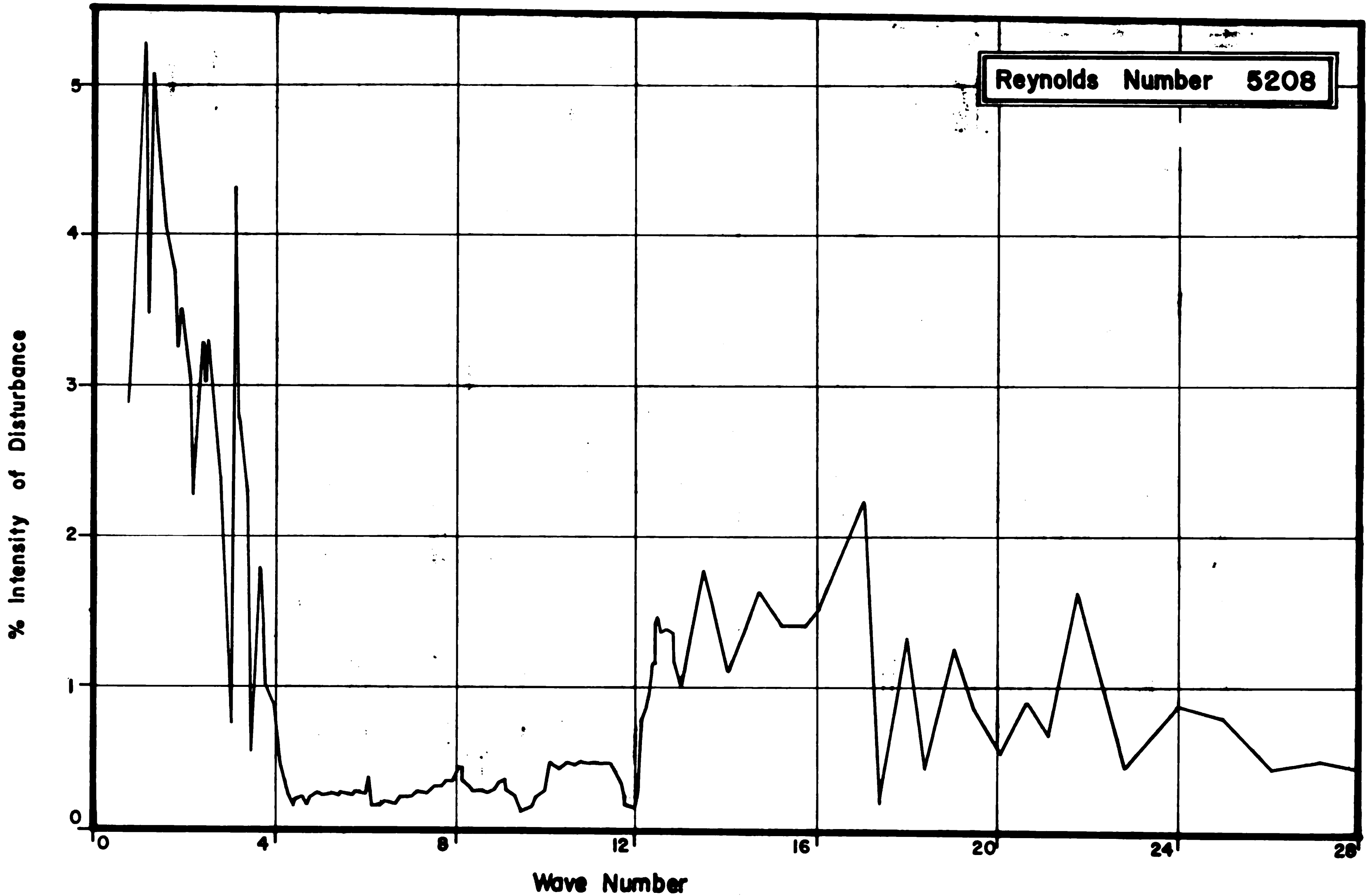

VARIATION OF INTENSITY WITH WAVE NUMBER FIG. 4.8

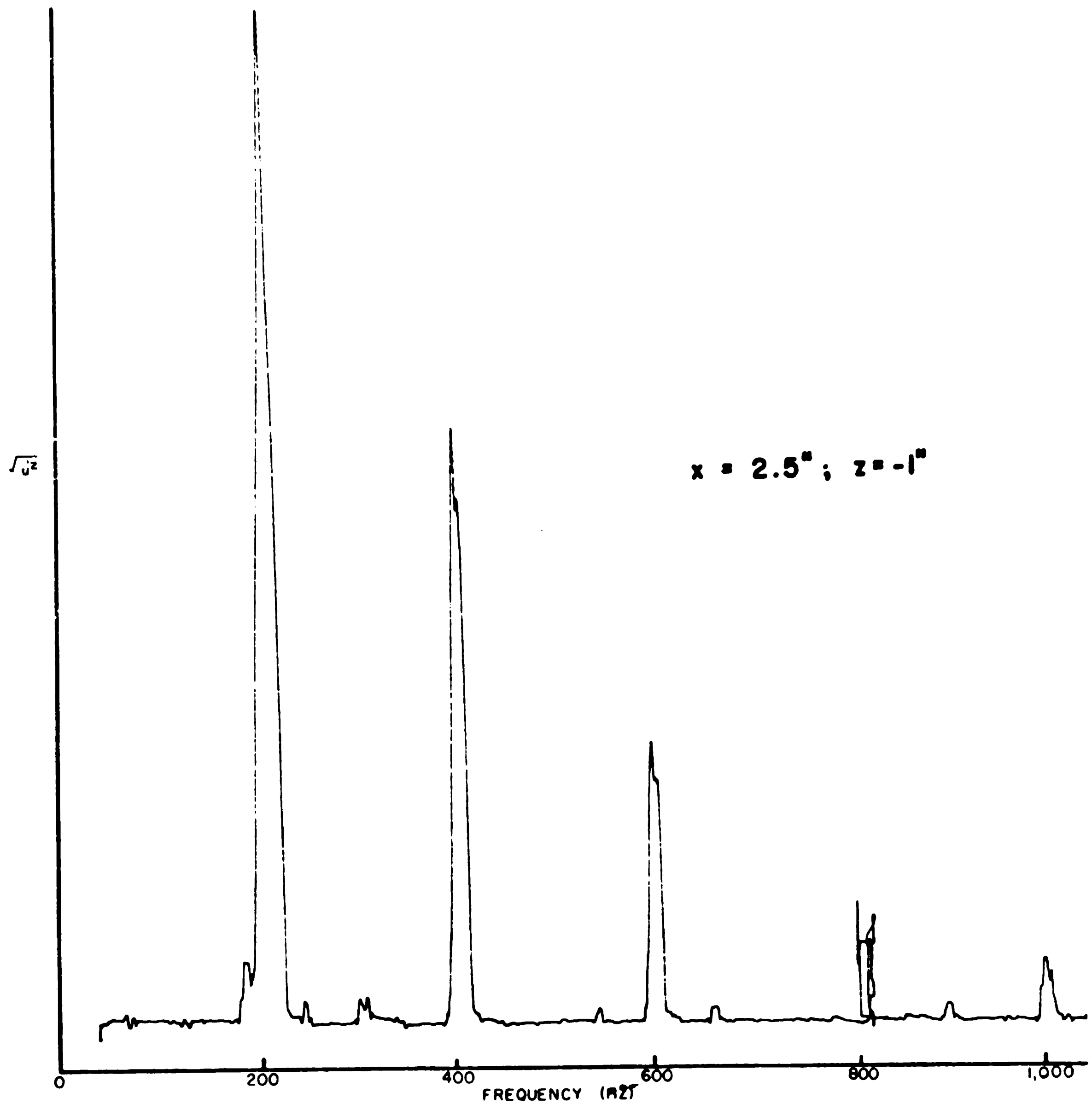

FREQUENCY SPECTRUM FIG. 4.9

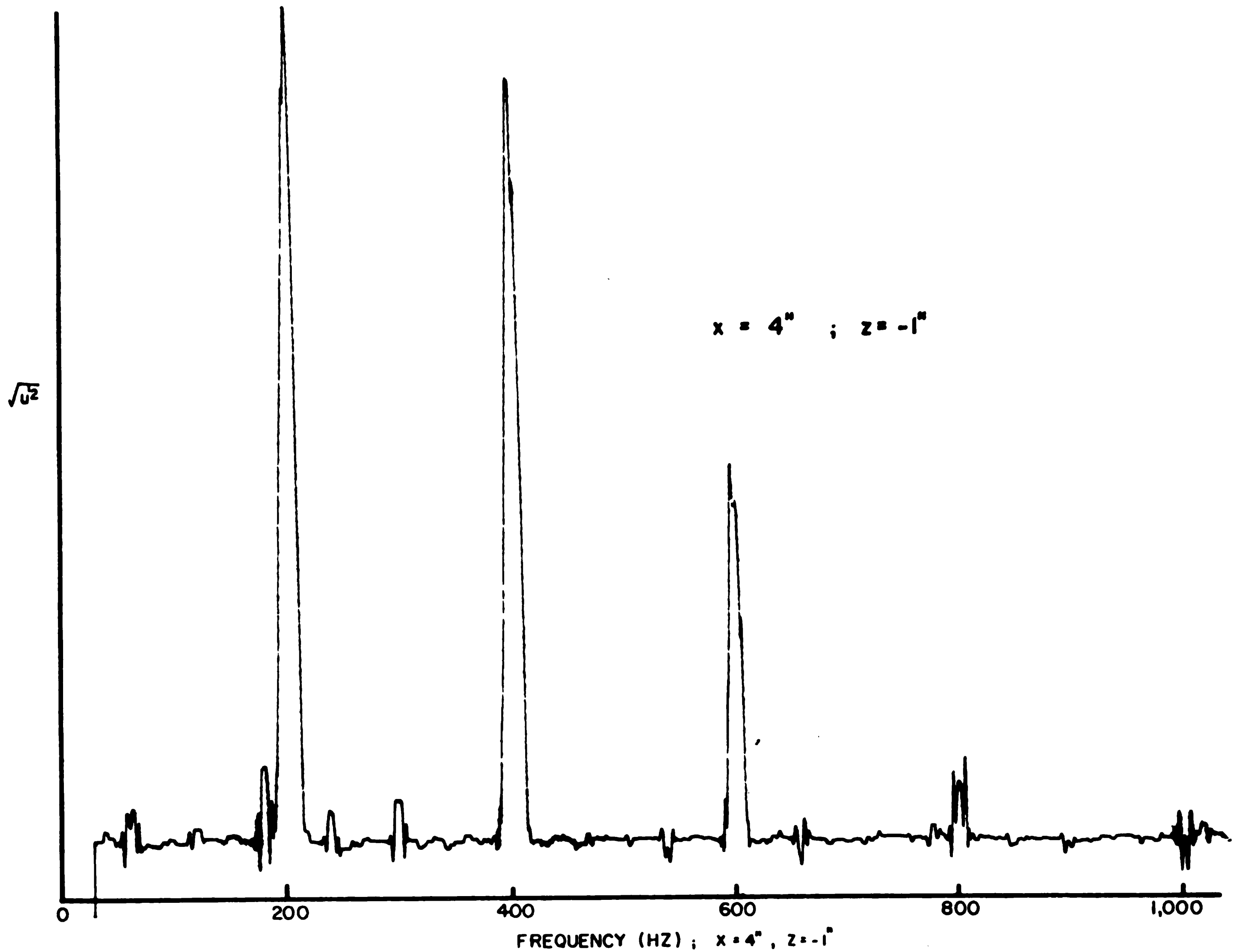

FREQUENCY SPECTRUM FIG. 4.10

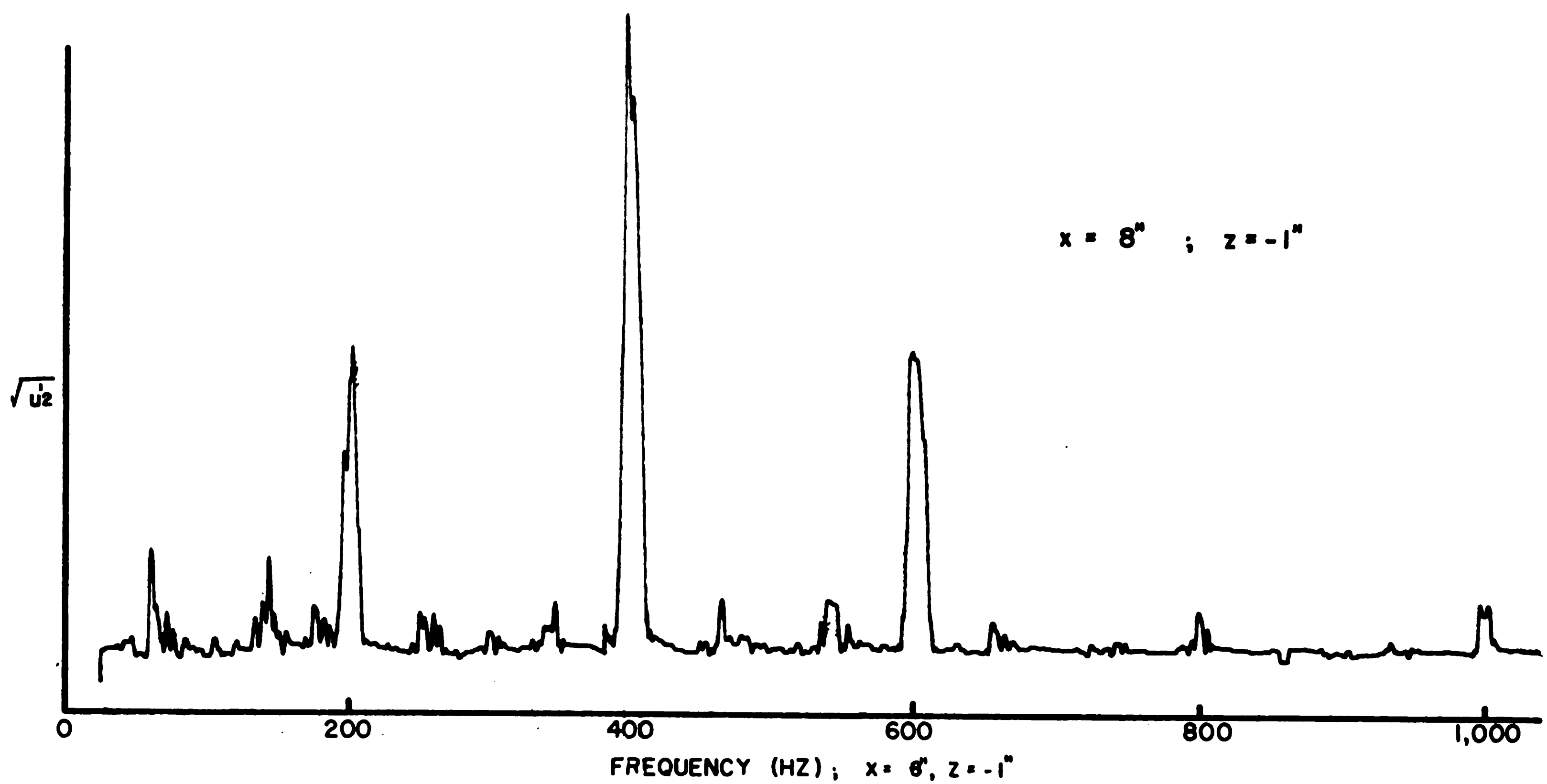

FREQUENCY SPECTRUM FIG. 4.11

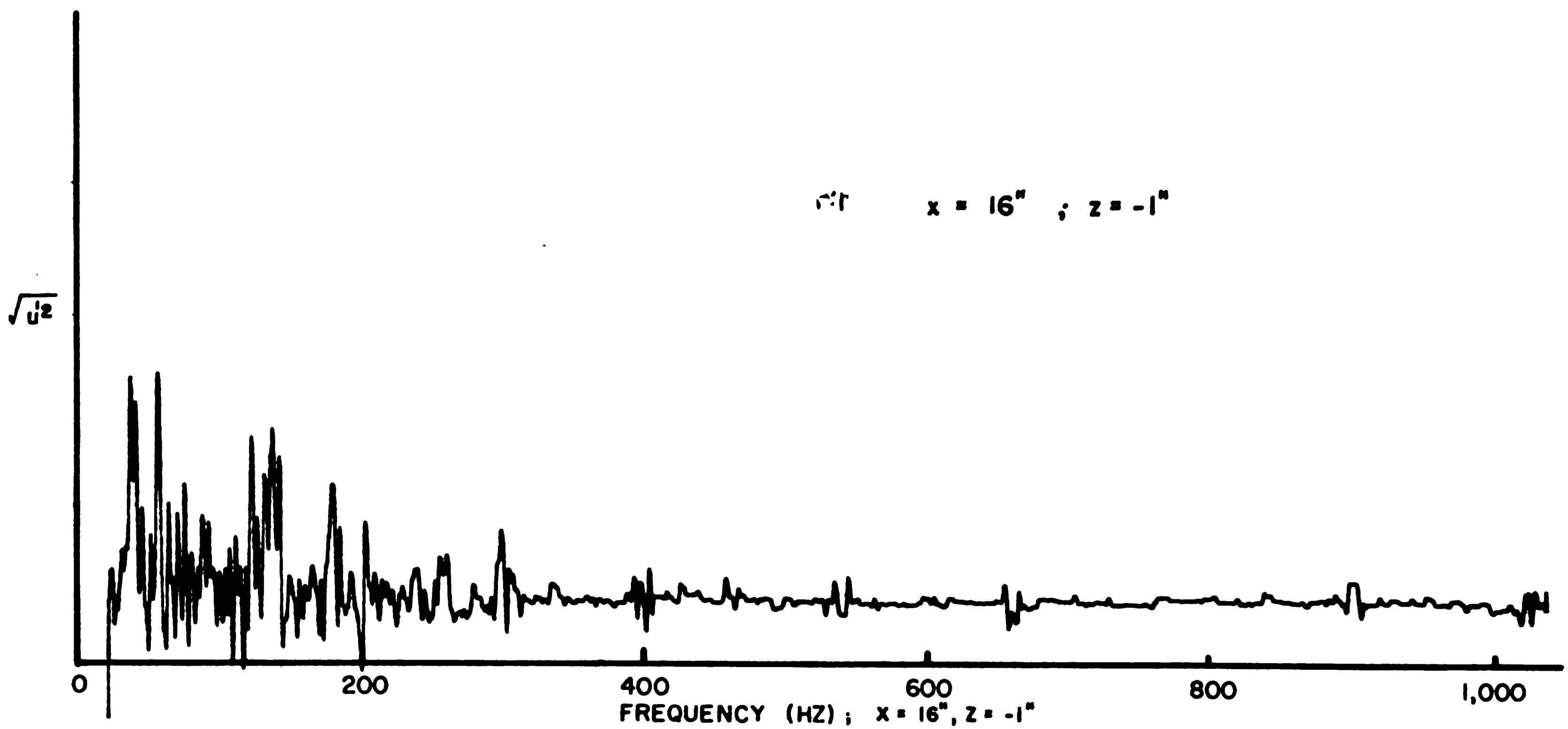

FREQUENCY SPECTRUM FIG. 4.12

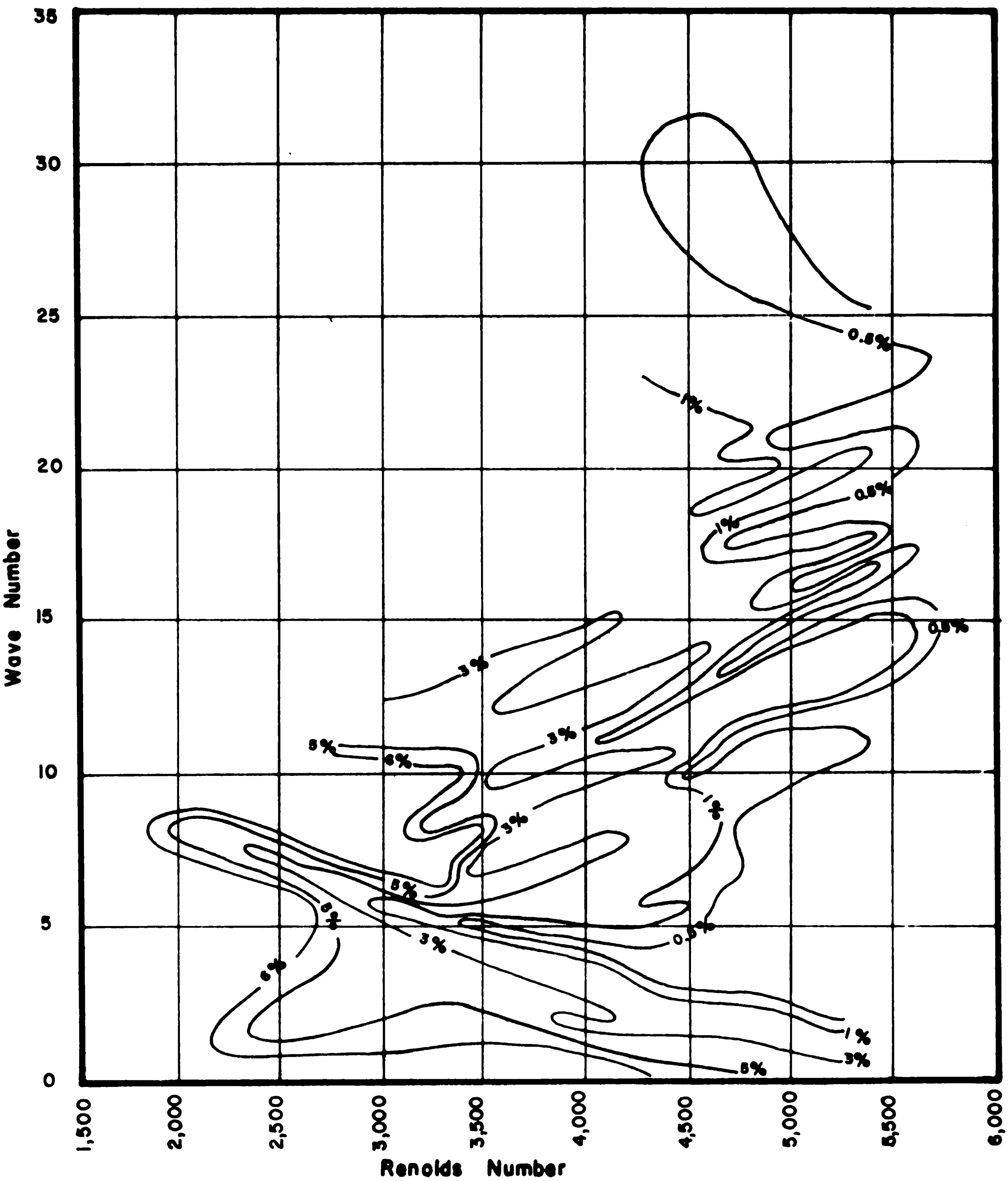

NEUTRAL STABILITY CURVES FIG. 4.13

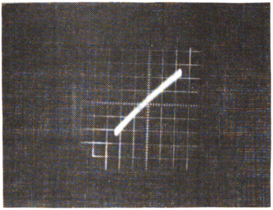

Stage 1

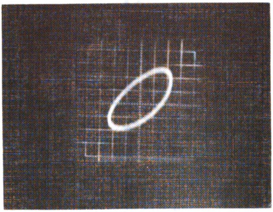

Stage 2

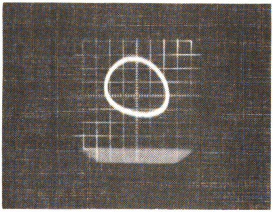

Stage 3

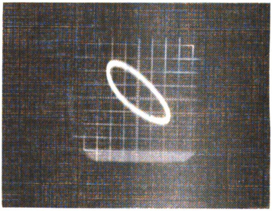

Stage 4

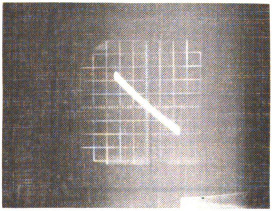

Stage 5

LISSAJOUS FIGURES FIG. 4.14

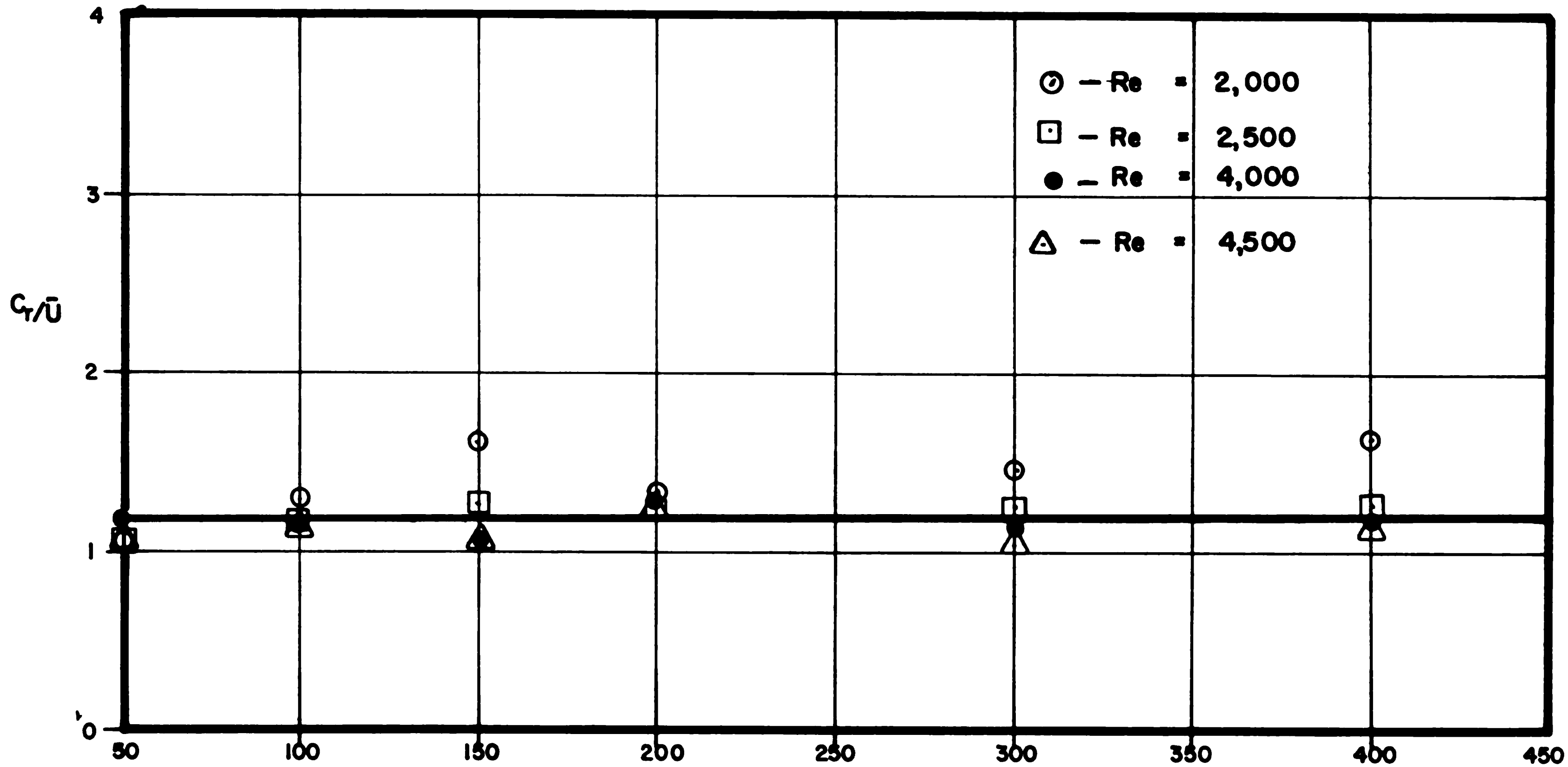

Frequency of Disturbance (hertz) FIG. 4.15

WAVE SPEED

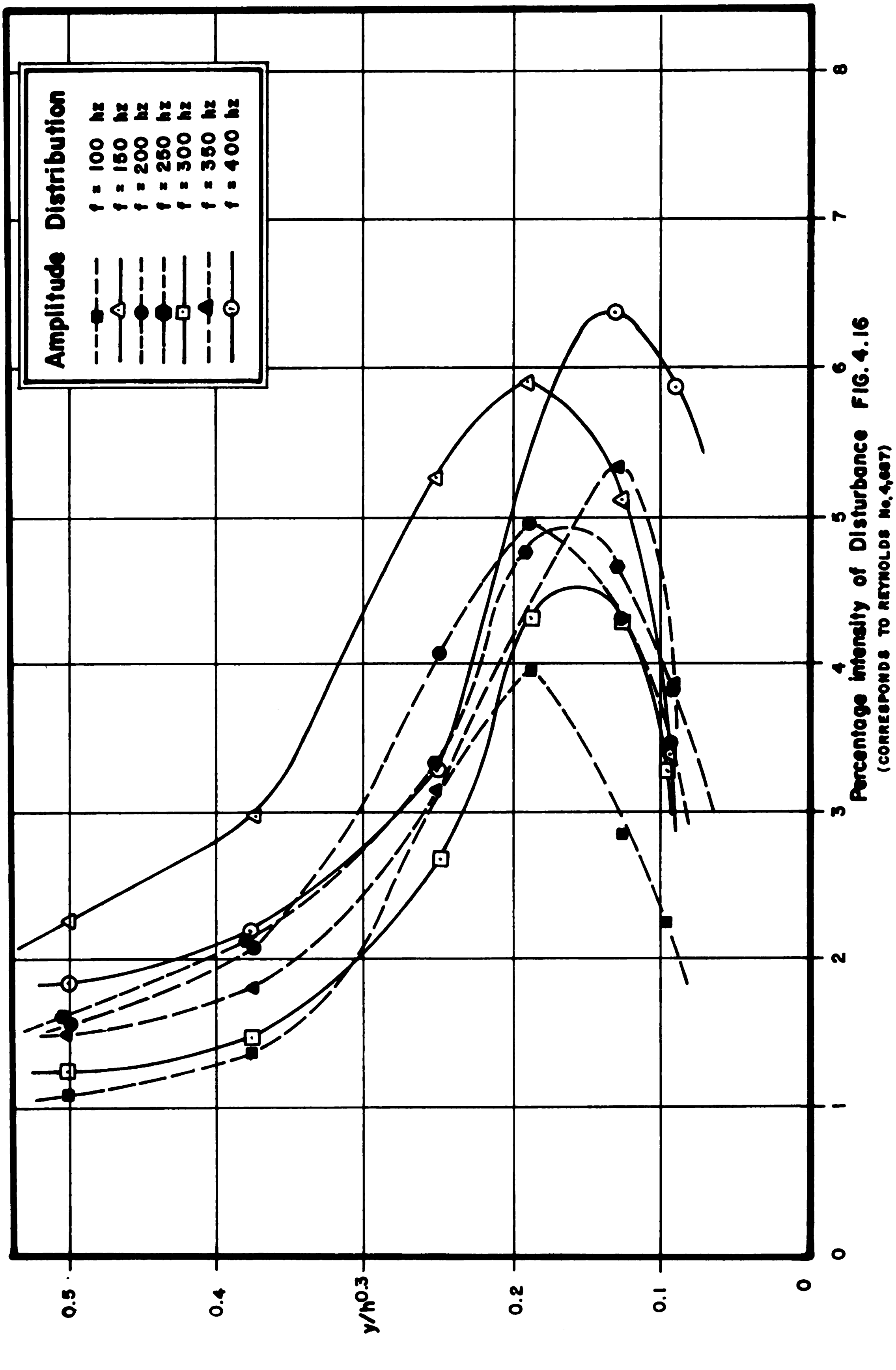

Amplitude Distribution
f = 100 hz
f = 150 hz
f = 200 hz
f = 250 hz
f = 300 hz
f = 350 hz
f = 400 hz
0.5
0.4
y/h^0.3
0.2
0.1
0
0
1
2
3
4
5
6
7
8
Percentage intensity of Disturbance
(CORRESPONDS TO REYNOLDS No. 4,687)

FIG. 4.16

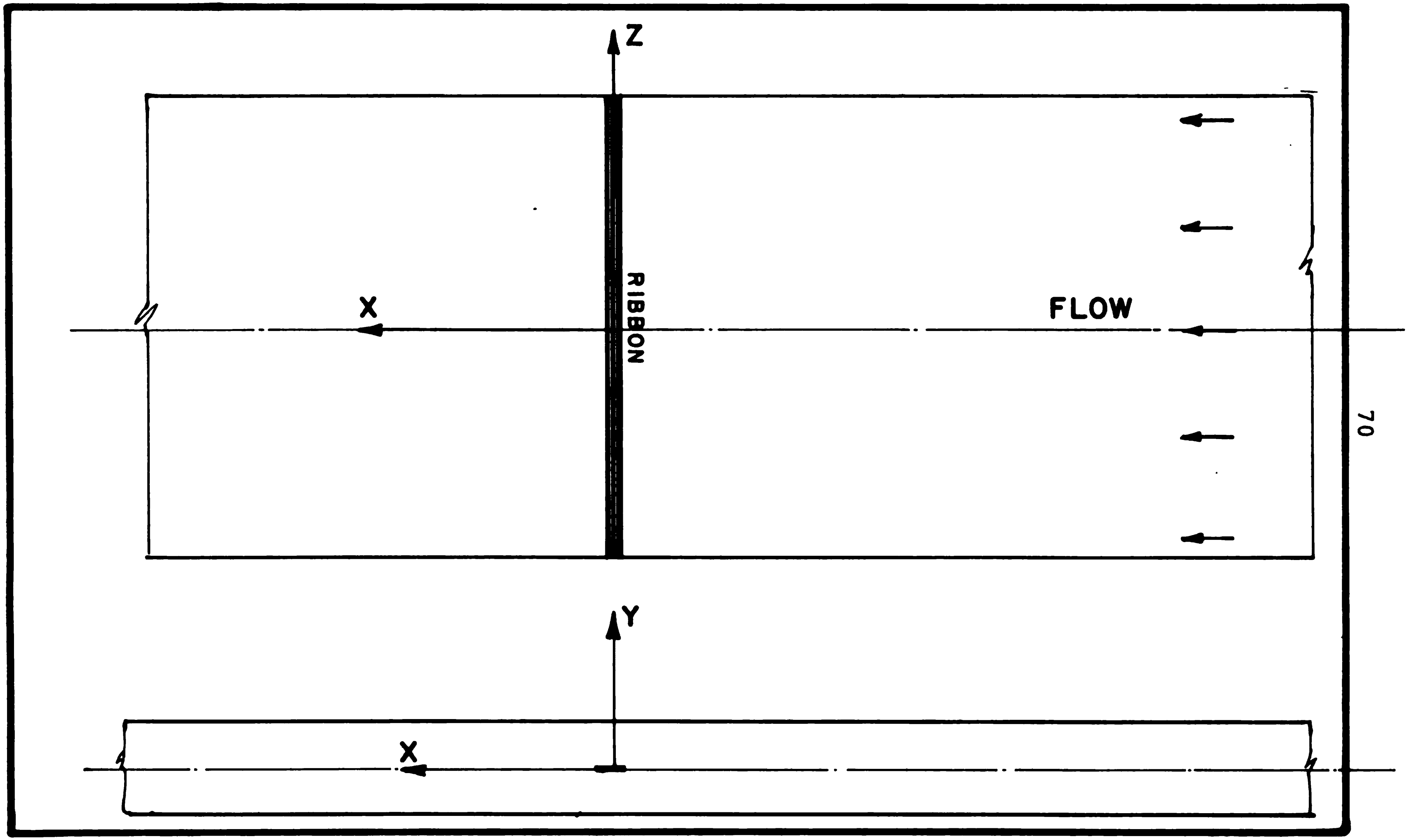

COORDINATE SYSTEM FOR THE CHANNEL FIG. 4.17

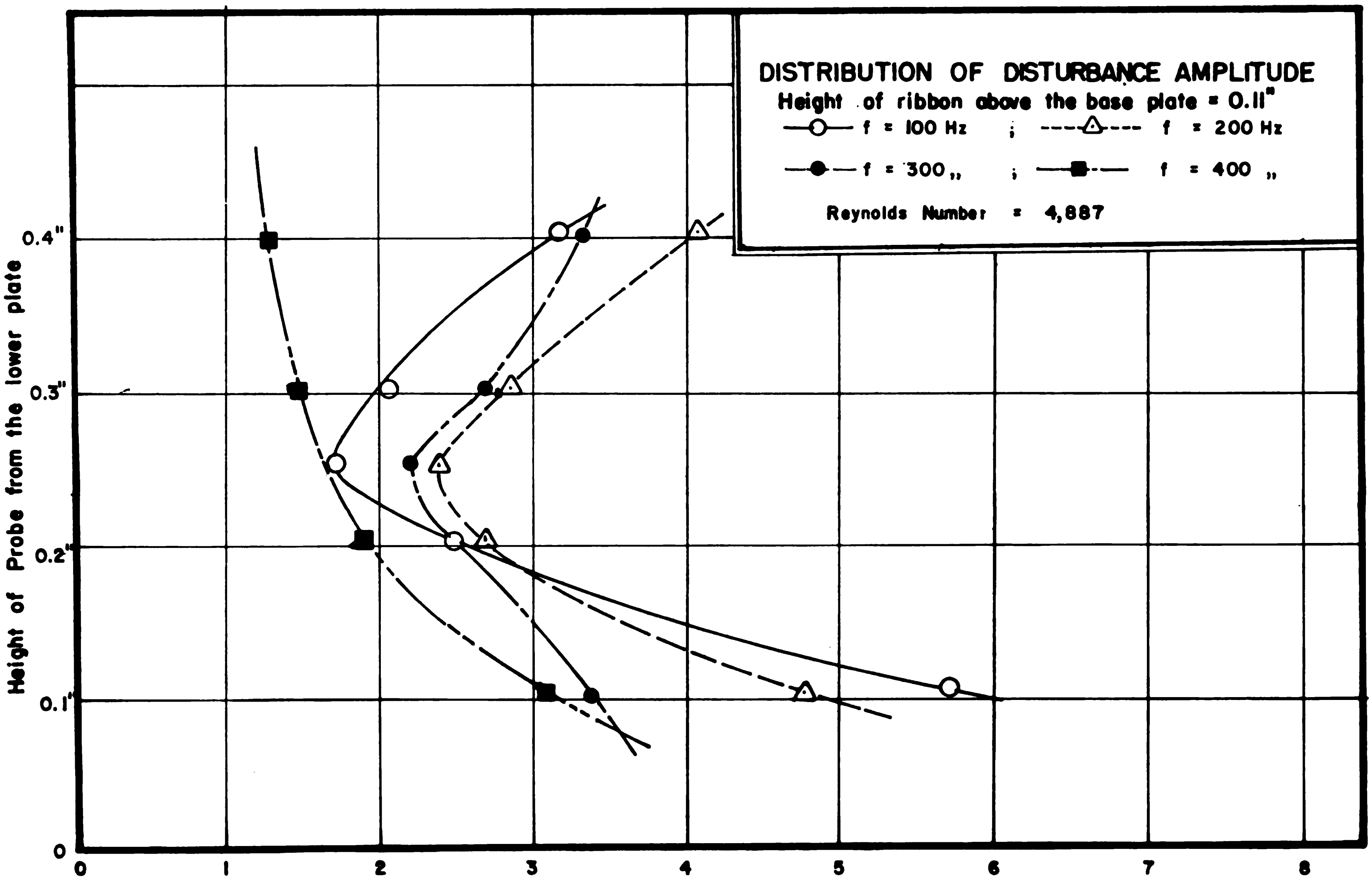

Percentage intensity of Disturbance FIG. 4.18

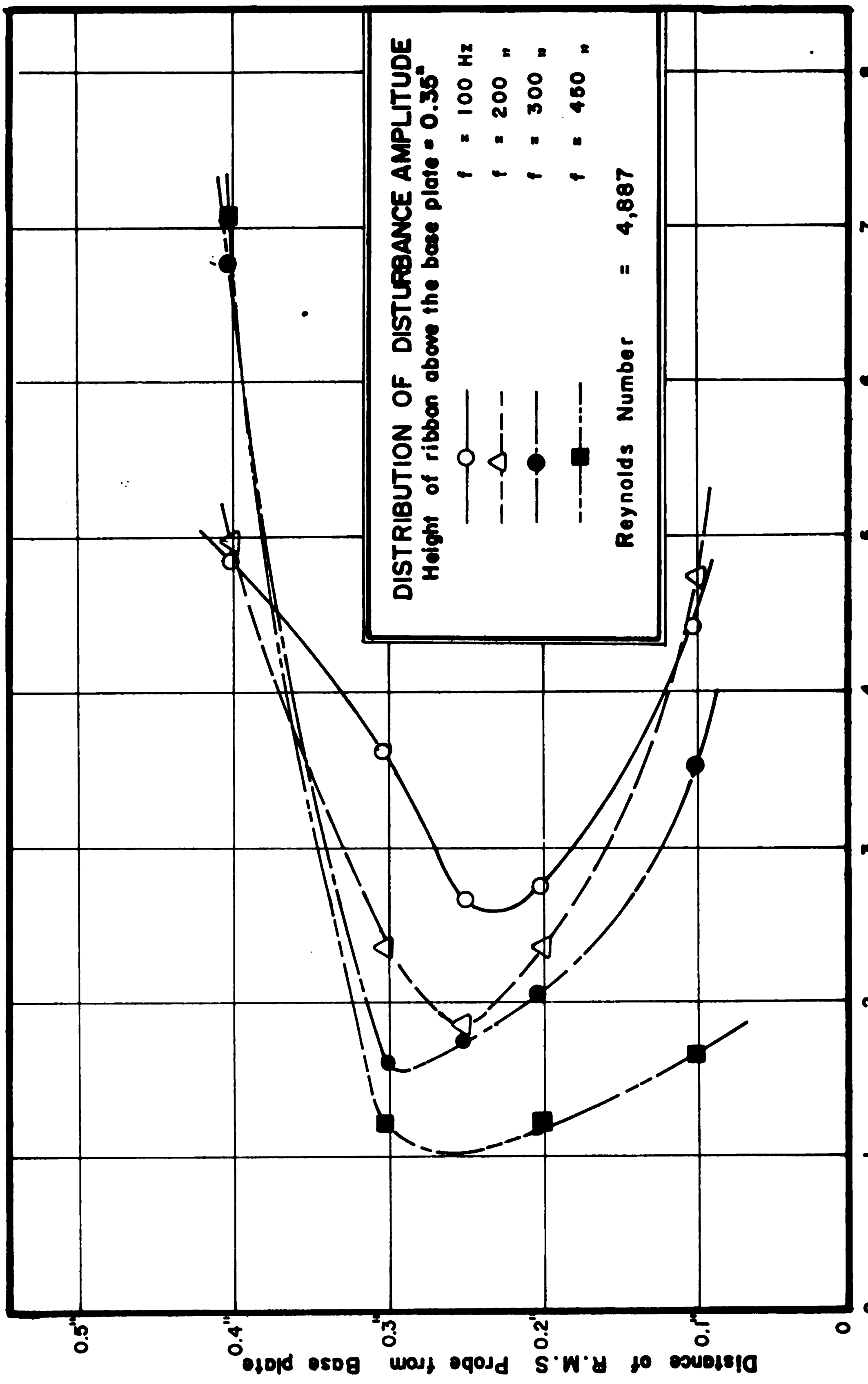

% Intensity of Disturbance FIG. 4.19

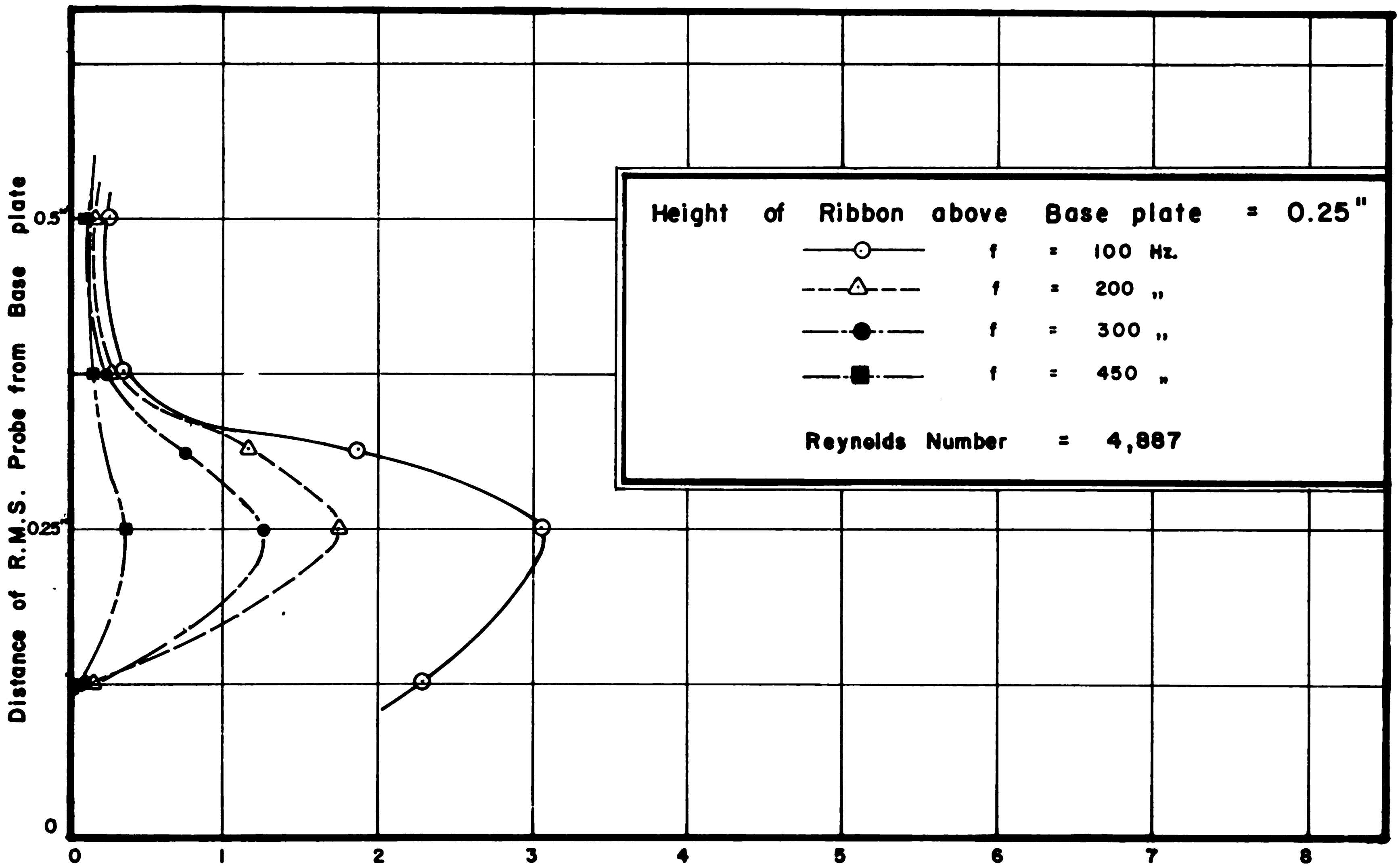

% Intensity of Disturbance FIG. 4.20

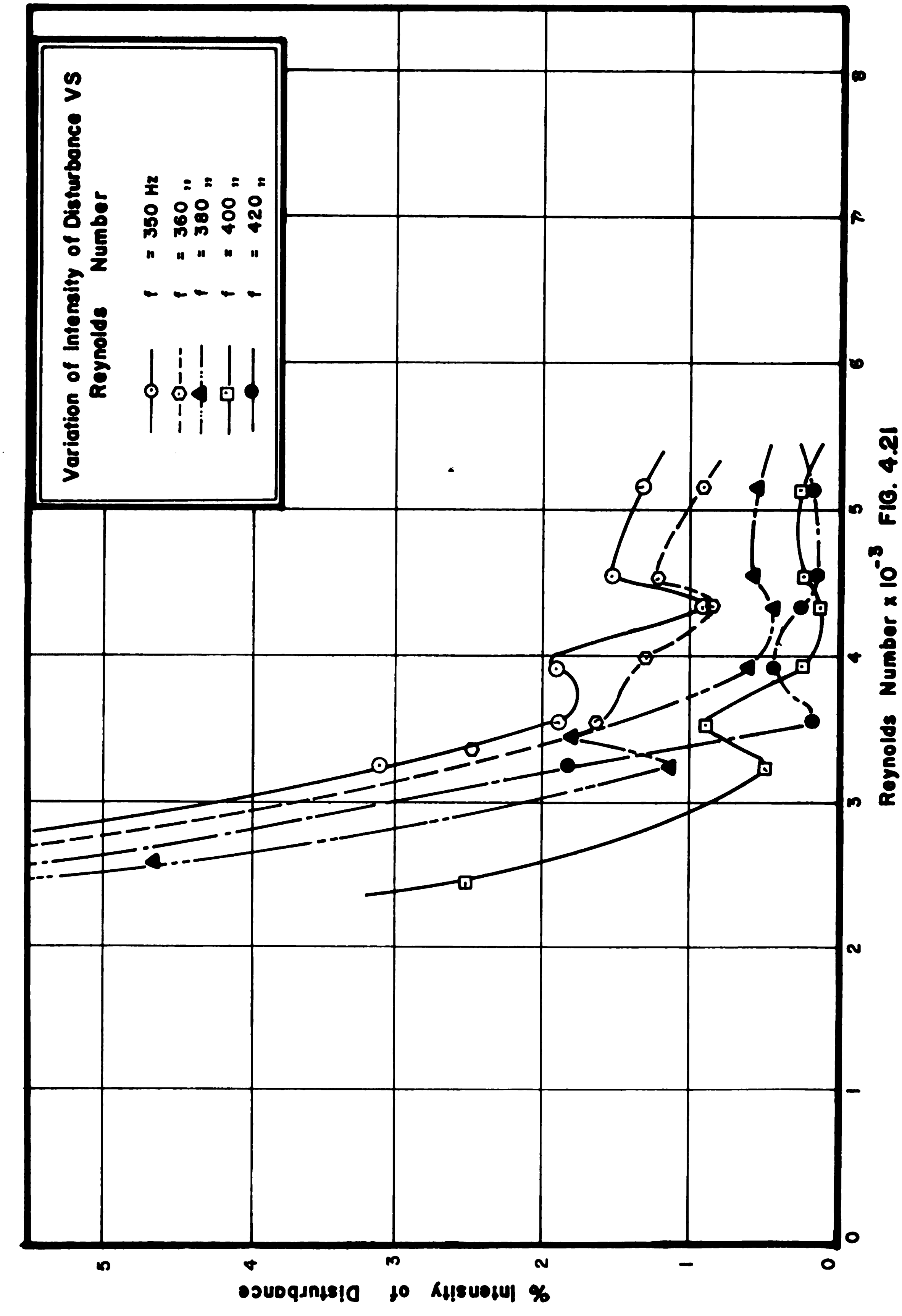

Variation of Intensity of Disturbance VS Reynolds Number
f = 350 Hz
f = 360 "
f = 380 "
f = 400 "
f = 420 "
Reynolds Number x 10^{-3}
% Intensity of Disturbance
0
1
2
3
4
5
6
7
8

FIG. 4.21

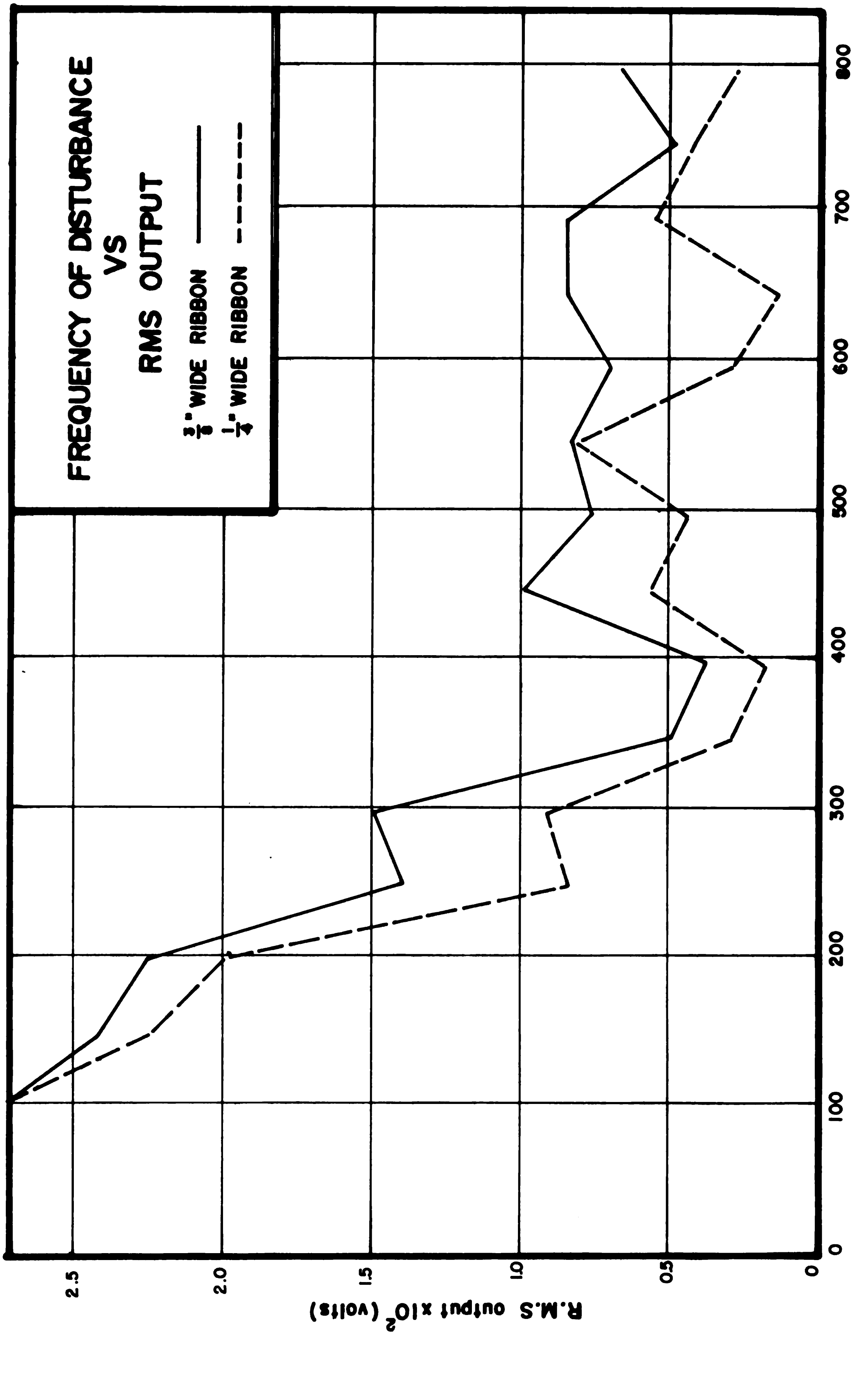

Frequency of disturbance (Hz) FIG. 4.22

LIST OF REFERENCES

LIST OF REFERENCES

1. Bradshaw, P., Stuart, J. T. and Watson, J. "Flow Stability in the Presence of Finite Initial Disturbances," AGARD Rept. 253 (1960).

2. Emmons, H. W. "The Laminar-Turbulent Transition in a Boundary Layer--Part I," J. Aero. Sci., 18, 490 (1951).

3. Feliss, N. A. Ph.D. dissertation, Michigan State University (1973).

4. George, W. D. and Hellums, J. D. "Hydrodynamic Stability in Plane Poiseuille Flow with Finite Amplitude Disturbances," J. Fluid Mech. 51, 687 (1972).

5. Heisenberg, W. "Über Stabilität und Turbulenz von Flüssigkeitsströmen," Ann. Phys., Lpz. 74, 577 (1924).

6. Hussain, A. K. M. F. and Reynolds, W. C. "The Mechanics of an Organized Wave in Turbulent Shear Flow." J. Fluid Mech. 41, 241 (1970).

7. Kao, T. W. and Park, C. "Experimental Investigation of the Stability of Channel Flows. Part 1. Flow of a Single Liquid in a Rectangular Channel," J. Fluid Mech. 43, 145 (1970).

8. Karnitz, N. A. Ph.D. dissertation, Michigan State University (1971).

9. Landau, L. "On the Problem of Turbulence," C. R. Academy of Sciences, U.S.S.R. 44, 311 (1944).

10. Lin, C. C. "The Theory of Hydrodynamic Stability," Cambridge University Press, London (1955).

11. McIntire, L. V. and Lin, C. H. "Finite Amplitude Instability of Second-Order Fluids in Plane Poiseuille Flow," J. Fluid Mech. 52, 273 (1972).

12. Meksyn, D. and Stuart, J. T. "Stability of Viscous Motion Between Planes for Finite Disturbances," Proc. Roy. Soc. A 208, 517 (1951).

13. Narayanan, M. A. B. and Narayana, T. "Some Studies on Transition from Laminar to Turbulent Flow in a Two-Dimensional Channel," Z. Angew. Math. Phys., 18, 642 (1967).

14. Noether, F. "Zusammenfassende Berichte Das Turbulenzproblem," Z. Angew. Math. Mech. 1, 125 (1921).

15. Pekeris, C. L. and Shkoller, B. "Stability of Plane Poiseuille Flow to Periodic Disturbances of Finite Amplitude," J. Fluid Mech. 39, 611 (1969a).

16. Pekeris, C. L. and Shkoller, B. "The Neutral Curves for Periodic Disturbances of Finite Amplitude of Poiseuille Flow," J. Fluid Mech. 39, 629 (1969b).

17. Pekeris, C. L. and Shkoller, B. "Stability of Plane Poiseuille Flow to Periodic Disturbances of Finite Amplitude, II," Proc. National Academy of Sciences, 68, 197 (1971).

18. Pekeris, C. L. and Shkoller, B. "Stability of Plane Poiseuille Flow to Periodic Disturbances of Finite Amplitude, III," Proc. National Academy of Sciences, 68 1434 (1971).

19. Reynolds, W. C. and Potter, M. C. "Finite Amplitude Instability of Parallel Shear Flows," J. Fluid Mech. 27, 465 (1967).

20. Schlichting, H. "Boundary Layer Theory," McGraw-Hill Book Co., Inc., New York (1968).

21. Sherlin, G. C. "Behaviour of Isolated Disturbances Superimposed on Laminar Flow in a Rectangular Pipe," J. Res. N.B.S. Sec. A, Phys. and Chem., 64A, 281 (1960).

22. Schubaur, G. B. and Skramstad, H. K. "Laminar Boundary Layer Oscillations and Transition on a Flat Plate," NACA Rept. No. 909 (1947).

23. Schubaur, G. B. and Klebanoff, P. S. "Contribution on the Mechanics of Boundary Layer Transition," NACA Rept. No. 1289 (1956).

24. Squire, H. B. "On the Stability for Three-Dimensional Disturbances of Viscous Fluid Flow Between Parallel Walls," Proc. Roy. Soc., London, A 142, 621 (1933).

25. Stuart, J. T. "On the Non-linear Mechanics of Hydrodynamic Stability," J. Fluid Mech. 4, 1 (1958).

26. Stuart, J. T. "On the Non-linear Mechanics of Wave Disturbances in Stable and Unstable Parallel Flows," J. Fluid Mech. 9, 353 (1960).

27. Thomas, L. H. "The Stability of Plane Poiseuille Flow," Physical Review, 4, 91 (1953).

28. Watson, J. "On the Non-linear Mechanics of Wave Disturbances in Stable and Unstable Parallel Flows," J. Fluid Mech. 9, 371 (1960).

29. Watson, J. "On Spatially-growing Finite Disturbances in Plane Poiseuille Flow," J. Fluid Mech. 14, 221 (1962).

30. Zahn, J. P. et al. "Non-linear Cellular Motions in Poiseuille Channel Flow," J. Fluid Mech. 64, 319 (1974).